ISTANBUL TECHNICAL UNIVERSITY ★ GRADUATE SCHOOL

RECOVERY OF VALUABLE METALS FROM WASTE LITHIUM-ION BATTERIES BY METALLURGICAL ROUTES

M.Sc. THESIS

Sepehr ABTAHI

Department of Metallurgical and Materials Engineering

Materials Engineering Programme

JUNE 2023

ISTANBUL TECHNICAL UNIVERSITY ★ GRADUATE SCHOOL

RECOVERY OF VALUABLE METALS FROM WASTE LITHIUM-ION BATTERIES BY METALLURGICAL ROUTES

M.Sc. THESIS

Sepehr ABTAHI
(506181427)

Department of Metallurgical and Materials Engineering

Materials Engineering Programme

Thesis Advisor: Prof. Dr. Onuralp YÜCEL

JUNE 2023

İSTANBUL TEKNİK ÜNİVERSİTESİ ★ LİSANSÜSTÜ EĞİTİM ENSTİTÜSÜ

ATIK LİTYUM-İYON PİLLERDEN DEĞERLİ METALLERİN METALURJİK YOLLARLA GERİ KAZANIMI

YÜKSEK LİSANS TEZİ

Sepehr ABTAHI
(506181427)

Metalurji ve Malzeme Mühendisliği Ana Bilim Dalı

Melzeme Mühendisliği Programı

Tez Danışmanı: Prof. Dr. Onuralp YÜCEL

HAZİRAN 2023

Sepehr ABTAHI, a M.Sc. student of ITU Graduate School student ID 506181427, successfully defended the thesis entitled "RECOVERY OF VALUABLE METALS FROM WASTE LITHIUM-ION BATTERIES BY METALLURGICAL ROUTES", which he prepared after fulfilling the requirements specified in the associated legislations, before the jury whose signatures are below.

Thesis Advisor: **Prof. Dr. Onuralp YÜCEL** ....
Istanbul Technical University

Jury Members: **Prof. Dr. Filiz ÇINAR ŞAHİN** ....
Istanbul Technical University

Assoc. Prof. Dr. Ahmet TURAN ....
Yalova University

Date of Submission : 15 June 2023
Date of Defense : 23 June 2023

FOREWORD

I would like to express my deep appreciation to Prof. Dr. Onuralp YÜCEL for his invaluable mentorship, guidance, and unwavering support throughout my research journey. His expertise and assistance have played a pivotal role in shaping the development of this master thesis.

I extend my profound gratitude to Assoc. Prof. Dr. Ahmet TURAN for his expert knowledge and guidance as my moderator. His contributions have been instrumental in providing direction and valuable insights for this work.

I am sincerely grateful to Prof. Dr. Filiz ŞAHİN for her empathetic support throughout my educational journey, particularly during challenging times. Her encouragement and guidance have been invaluable to my personal and academic growth.

I would like to dedicate my warmest gratitude to Research Assistant Kağan BENZEŞİK for his sincere and selfless support, which has been a crucial factor in the successful completion of this project. His dedication and assistance have greatly contributed to the overall quality and achievement of this work.

I extend my heartfelt thanks to Research Assistant Selçuk KAN for his consistent availability and assistance throughout our research journey. His collaboration and contributions have significantly enhanced the progress and outcomes of this study.

Lastly, I would like to express my special thanks to Mr. Hassan, a master's student, for his invaluable assistance with the induction furnace and his unwavering support throughout this project. His contributions have been indispensable to the successful execution and accomplishments of our work.

June 2023

Sepehr ABTAHI
(Metallurgical and Materials Engineer)

TABLE OF CONTENTS

Page

ABBREVIATIONS

BET	**:** Brunauer-Emmett-Teller
BF	**:** Blast Furnace
BOF	**:** Basic Oxygen Furnace
CCS	**:** Carbon Capture and Storage
EAF	**:** Electric Arc Furnace
GHG	**:** Greenhouse Gas
IGCC	**:** Integrated Gasification Combined Cycle
PSA	**:** Pressure Swing Adsorption
TGA	**:** Thermogravimetric Analysis
TSA	**:** Temperature Swing Adsorption
UNFC	**:** United Nations Framework Convention on Climate Change
XRD	**:** X-ray Diffraction

SYMBOLS

#	**:** Number sign
%	**:** Percent sign
°C	**:** Celsius
g	**:** Gram
m	**:** Metre
m^2	**:** Metre square
mm	**:** Millimetre
µm	**:** Micrometre

LIST OF TABLES

Page

LIST OF FIGURES

Page

RECOVERY OF VALUABLE METALS FROM WASTE LITHIUM-ION BATTERIES BY METALLURGICAL ROUTES

SUMMARY

This master's thesis aims primarily to develop a selective method for extracting vital metals from depleted lithium-ion batteries (LIBs). These include lithium, cobalt, nickel, copper, and manganese. Initially, the thesis explores the prevailing literature on the subject. Subsequently, two methods are selected for thorough investigation: hydrometallurgical leaching with hydrochloric acid and pyrometallurgical processing through induction and ash furnace smelting and roasting.

The hydrometallurgical route employs segregated electrode materials derived from LIBs, which undergo leaching in a hydrochloric acid solution for a two-hour duration at an average temperature of 85.5 ºC. Post-leaching, the samples are analyzed using atomic absorption spectrometry, revealing the samples to contain fluctuating quantities of Mn, Cu, Ni, and Co, dependent on the dilution factor.

The pyrometallurgical route subject's electrode samples to roasting at rising temperatures ranging from 700 ºC to 1500 ºC over spans of 1 to 3 hours. The findings from these experiments suggest that the primary elements extracted from the LIBs are Mn, Cu, Ni, and Co. It was established that by quickly elevating the temperature to a range between 1250 – 1350 ºC, direct metallic conversion of the valuable elements could be attained. Additionally, to mitigate any adhesive interaction between the sample and the ceramic crucible and to ensure a fully smelted sample, flux materials - silicon dioxide (silica) and sodium borate (borax) were utilized.

The initiation of the experimental operation involved the sample undergoing smelting at a predetermined temperature spectrum of 1350 – 1400 °C, supplemented by a 15% carbon contribution. Sequential trials maintained the same temperature range while adjusting the carbon supplement's proportion and typology for optimizing the carbothermic reduction reaction. The resultant sample's elemental composition comprised a dominant 95% Mn, with 2% each of Cu and Co, and 1% Ni. The recovery rates, calculated from Table 5.6, for these metals in their metallic forms were: a substantial 65% for Mn, 52% for Co, and a notable 69% for Ni. A key observation was the 75% recovery rate of Mn in the metallic fraction, marking a significant advancement in the extraction process.

In conclusion, the thesis finds the recovery of valuable metals from exhausted LIBs through metallurgical routes a promising technique. Both the investigated methods - hydrometallurgical leaching and pyrometallurgical processing, indicate the feasibility of significant metal recovery. Nevertheless, ongoing research is necessary to further refine the process and enhance its efficacy for large-scale applications. Overall, the thesis successfully illustrates the potential of recovering valuable metals from discarded lithium-ion batteries through metallurgical paths, contributing valuable insights for future research in this domain.

ATIK LİTYUM-İYON PİLLERDEN DEĞERLİ METALLERİN METALURJİK YOLLARLA GERİ KAZANIMI

ÖZET

Lityum-iyon pilleri (LIB) son yılların en popüler enerji depolama sistemi olmuştur. Ancak, kullanım ömrünün sonunda atılan pillerin sayısı hızla artmaktadır ve bu atıkların geri dönüştürülmesi önem kazanmıştır. Bu tezde, Li, Co, Ni ve Mn gibi metallerin geri dönüştürülmesi için farklı yöntemler ve teknikler incelenmiştir. Özellikle, hidrometalurji ve piroliz yöntemleri üzerinde durulmuştur. Ayrıca, bu metallerin geri kazanımı için kullanılan asitlerin etkileri ve optimal koşullar analiz edilmiştir. Bu çalışma, atık LIB lerin geri dönüştürülmesinde yeni yollar ve fikirler sunacaktır.

Dünya çapındaki LIB pazarı, elektrikli araçlar ve yenilenebilir enerji depolama sistemleri talebindeki artış nedeniyle gelecek yıllarda hızla büyümeye devam edecektir. MarketsandMarkets'in son raporuna göre, dünya çapındaki LIB pazarı 2025 yılına kadar $93.1 milyar dolara ulaşacak ve bu tahmini dönemde yıllık %17,5 yıllık bileşik büyüme oranı ile büyüyecektir.

Elektrikli araçların (EV'lerin) talebindeki artış, LIB pazarının en önemli itici gücüdür. EV'lerin kullanımı, karbon emisyonlarını azaltmaya ve hava kalitesini iyileştirmeye yönelik ihtiyaç nedeniyle artmaktadır. Dünya çapında hükümetler, finansal teşvikler ve düzenlemeler aracılığıyla EV'lerin kullanımını teşvik etmektedir. Bu nedenle, sokaklardaki EV sayısı gelecek yıllarda önemli ölçüde artacak ve bu LIB talebindeki artışa yol açacaktır.

LIB piyasasının başka bir önemli bileşeni, enerji depolama sistemleri için artan taleptir. Güneş ve rüzgar gibi yenilenebilir enerji kaynaklarının kullanımının artması, enerji depolama sistemlerine olan ihtiyacı arttırmıştır. LIB'ler, yüksek enerji yoğunluğu, uzun kullanım ömrü ve düşük kendiliğinden boşalma oranları nedeniyle enerji depolama uygulamaları için uygundur.

Türkiye'de, dünya pazarı gibi, lityum-iyon pillerin kullanımı da çeşitli alanlarda artmaktadır. Türkiye'de temel kullanım alanları, elektrikli araçlar ve hibrit elektrikli araçlar ile enerji depolama sistemleri dahil olmak üzere ulaştırmadır. Türkiye, yenilenebilir enerji kaynaklarının ve elektrikli araçların kullanımını teşvik etmeye yönelik politikalar uygulamıştır, bu da ülkede LIB talebini arttırmaktadır. Elektrikli araçların ve yenilenebilir enerji depolama sistemlerinin talebinin artması, Türkiye'de LIB pazarının büyümesini hızlandırmaktadır.

Türkiye'nin 2019 yılında açıkladığı Milli Enerji ve Maden Politikası, 2023 yılına kadar yenilenebilir enerjinin enerji üretimindeki payını %30'a çıkarmayı amaçlamaktadır. Bu, yenilenebilir enerji kapasitesinin önemli ölçüde genişletilmesini gerektirecektir ve bu da aynı zamanda dolaylı olarak Lityum İyon Piller pazarının büyümesine neden olacaktır.

Atık Li-iyon piller, metallerinin geri dönüşümü, çevre ve enerji kaynaklarının korunmasına katkıda bulunabilecek niteliktedir. Madencilikten kaynaklanan sera gazı emisyonlarını azaltmak, doğal kaynakları korunması ve nakliyeye ihtiyacı azaltmak en önemli çevresel faydalarındandır. Ayrıca, atık Li-iyon pillerin metallerinin geri dönüşümü, atık miktarını azaltır ve bu da çevreye pozitif etkiler yaratabilir.

Ayrıca, atık LIB'lerden metal çıkarmanın, yeşil enerji ekonomisi gelişimine de katkıda bulunabileceği de vurgulanmalıdır. Özellikle, lityum, EV'lerde ve yenilenebilir enerji depolama sistemlerinde enerjiyi saklamak ve aktarmanın kullanıldığı LIB'lerin üretiminde esastır. Atık LIB'lerden lityum elde etmenin, litiyum için yabancı kaynaklara bağımlılığı azaltmasına ve daha sürdürülebilir bir enerji sistemi oluşturmasına yardımcı olması beklenilmektedir.

Atık LIB'lerden kobalt, nikel ve lityum metallerinin geri dönüşümü önemlidir, çünkü ekonomimiz için önemli olan, ancak sınırlı bir tedariğe sahip olan metaller olarak kabul edilirler. Bu metalleri atık LIB'lerden elde etmek, kaynakları korumaya ve yerli üretimi teşvik etmeye yardımcı olacaktır, daha dayanıklı ve sürdürülebilir bir enerji sistemi oluşmasına yol açacaktır.

Özetle, atık Li-ion pil (LIB)lerinden değerli metallerin kazanılması sadece kaynakları korumakla kalmaz, aynı zamanda çevreye olumlu etki yapar. Atık LIB'lerden metallerin geri dönüşümü sera gazı emisyonlarını azaltır, madencilik ve taşımacılık ihtiyacını azaltır ve atıkların depolandığı çöplükleri azaltır. Ayrıca, atık LIB'lerden metallerin çıkarılması, yabancı kaynaklardan bağımsız hale gelinmesi ve diğer kritik metallerin üretimini teşvik edilmesi yoluyla yeşil enerji ekonomisinin geliştirmesine katkıda bulunabilir. Sürdürülebilir ve dayanıklı bir enerji sistemi oluşturmak için atılması gereken önemli bir adımdır.

Bu yüksek lisans tezinin ana odak noktası, kullanılmış lityum-iyon pillerden (LIB'ler) lityum, kobalt, nikel, bakır ve manganez gibi değerli metallerin metalurjik yollar kullanılarak geri kazanılması için bir süreç geliştirmektir. Tez, konuyla ilgili mevcut literatürün gözden geçirilmesiyle başlamakta, ardından daha sonraki araştırma için iki yöntem seçilmektedir: hidroklorik asit ile hidrometalurjik liç, endüksiyon ve kül fırınlarında döküm ve pişirme yoluyla pirometalurjik proses.

Hidrometalurjik yöntem, LIB'lerden alınan ve daha sonra ortalama 85,5 ºC sıcaklıkta 2 saat boyunca hidroklorik asit çözeltisinde süzülen ayrılmış elektrot malzemelerinin kullanılmasını içermekteydi. Liç işleminden sonra numuneler atomik absorpsiyon spektroskopisi kullanılarak analiz edilmiş, bu da numunelerin seyreltme faktörüne bağlı olarak değişen miktarlarda Mn, Cu, Ni ve Co içerdiğini ortaya koymuştur.

Pirometalurjik yöntemde, elektrot numuneleri 1 ila 3 saatlik süreler boyunca 700 ºC ila 1500 ºC arasında artan sıcaklıklarda piroliz işlemine tabi tutulmuş / ergitilmiştir. Bu deneylerden elde edilen sonuçlar, LIB'lerden elde edilen ana elementlerin Mn, Cu, Ni ve Co olduğunu ortaya koymuştur. Sıcaklığın 1250 - 1350 ºC arasında belirli bir dereceye kadar hızla artırılmasıyla değerli elementlerin doğrudan metalik şekilde toplandığı tespit edilmiştir. Ayrıca, tamamen erimiş bir numuneye sahip olmak için flaks malzemesi olarak silika (silisyum dioksit) ve boraks (sodyum boraks dekahidrat) kullanılmıştır.

Ergitme deneyleri, belirlenen sıcaklık aralığı olan 1350 – 1400 °C'de yapılan işlemleri ve %15'lik bir karbon katkısıyla redüksiyon çalışmalarını içermiştir. Ardışık deneyler, karbon indirgeme reaksiyonunu optimize etmek için karbon katkısının oranını ve türünü ayarlayarak aynı sıcaklık aralığında gerçekleştirilmiştir. Örnek olarak, %95

Mn, %2 Cu, %2 Co ve %1 Ni içeren metalik fraksiyonlar elde edilmiştir. Metalik fraksiyonda Mn için %75'e varan geri kazanım oranlarına çıkılmıştır.

Sonuç olarak, bu tez çalışması, kullanılmış LIB'lerden değerli metallerin metalurjik yollarla geri kazanımının umut verici bir teknik olduğunu göstermiştir. İncelenen her iki yöntem - hidrometalurjik liç ve pirometalurjik işlem, metalin önemli miktarda geri kazanılabilirliğinin olası olduğunu göstermektedir. Ancak, süreci daha da optimize etmek ve büyük ölçekli uygulamalar için etkinliğini artırmak amacıyla devam eden araştırmalar gereklidir.

1. INTRODUCTION AND SCOPE

1.1 Background on Lithium-Ion Batteries and Their Increasing Use in Consumer Electronics and Electric Vehicles

There is a growing need for environmentally friendly energy sources and an improved quality of life as our society and industries rapidly progress. This trend has emphasized the shift towards sustainable development for the environment.

The development of lithium-ion batteries (LIBs) has had a significant positive impact on the pollution caused by petroleum-based fuels and on energy shortages. LIBs have also proven to be a suitable substitute for certain newer energy sources that have uncertain or inconsistent characteristics, such as tidal, solar, hydroelectric, nuclear, and wind power.

Lithium-ion batteries (LIBs) are a very promising energy source because of their high operating voltage, high specific energy, high power density, and extended cycle life. As a result, the market value of LIBs on a global scale is rising quickly, and methods for managing LIBs after the end of their useful lives are becoming more and more significant.

By 2030, industry researchers estimate that the annual global generation of wasted LIBs would be greater than 2 million tons and may perhaps exceed 4 million tons. Because LIBs include heavy metals and toxic electrolytes, improper handling of LIBs—such as disposal in a landfill or burning them—can be hazardous to the environment and to people's health. Recycling LIB parts has considerable positive effects on society and the environment. It also aids in reducing environmental contamination. Spent LIBs typically contain 5-10% nickel, 5-7% lithium, 5-7% cobalt, 5-20% manganese, 5-10% other metals (including copper, aluminum, iron), 15% organic compounds, and 7% plastic components.

In addition to addressing environmental issues related to the improper disposal of waste battery materials, the recovery of valuable components from spent LIBs can generate financial gains and environmental benefits by preventing the extraction of these components from virgin resources and ensuring a steady supply of raw materials for the manufacture of new batteries and other high-value applications.

Recycling LIBs is therefore necessary from resource, economic, and environmental perspectives, as well as for addressing supply risks for certain elements and reducing material costs. It is crucial for guaranteeing the circular potential of batteries, insuring the sustainable manufacture of LIBs, preserving natural resources, and minimizing environmental effects.

The lithium-ion battery (LIB) has evolved from the lead battery, which was invented in 1859. Sony began developing LIBs in 1986, and they were first commercialized in 1991[1]. At first, only specialized markets or small electronic equipment used these batteries. Their usage has, nevertheless, grown as a result of various factors.

The societal shift toward digitalization has raised the need for LIBs in handheld electronics like phones, laptops, and computers. Sales of smartphones reached 1.55 billion in 2018.Since LIBs are utilized in stationary storage to offset the intermittent nature of renewable energy sources and preserve grid stability, the switch to low-carbon energy has also raised demand for LIBs. LIBs are also used in electric and hybrid vehicles to reduce carbon dioxide emissions [2].

With a predicted 2.1 million more sales in 2019, the global stock of EVs is expected to increase to 5.1 million from the 2 million sold in 2018. The largest market is China, however the EU made up 1.2 million of the world's vehicle stock and sold 385,000 vehicles in 2018. The International Energy Agency predicts that by 2030, there will be a stock of 130–250 million electric vehicles, with sales rising to 23–40 million [3].

1.2 Global LIB Manufacturing and Trade

Starting with the decade 2010-2020, the demand for LIBs saw an impressive surge, primarily due to the rise in consumer electronics and electric vehicle markets. This period was characterized by significant technological advancements in LIB, leading to increased energy density and reduced costs. In 2020, the annual production of lithium stood at 364,000 tonnes/yr. China, with 45% of global lithium refining capacities, and Chile and Argentina, dominating brine operations, held significant sway in lithium supply.

Similarly, for cobalt, the Democratic Republic of Congo led production while China dominated the refining. The continued rise in demand for LIBs in the early 2020s has led to a boost in the global production capacity of LIBs. Production is predicted to rise from 950 GWh/yr in 2021 to 2000 GWh/yr in 2023. This production is heavily concentrated in Asia, with China contributing 66% of the finished LIBs. Looking ahead, substantial growth is expected in LIB production capacities, projected to exceed 3400 GWh/yr by 2027. The annual production of lithium and cobalt is estimated to reach nearly 1.59 million tonnes and 300,000 tonnes respectively by 2030. With new investments and manufacturing technologies maturing, we anticipate more investors to contribute to LIB production facilities. trends indicate a continued rise in demand for LIBs towards 2050, fueled by the proliferation of electric vehicles and renewable energy storage solutions.

The challenges anticipated in this period revolve around securing a stable supply of key materials, scaling up manufacturing capabilities, and managing the environmental and social impacts of increased production. Furthermore, enhanced recycling efforts will be critical to meeting material demands and mitigating environmental impacts.

Overall, the global LIB market is poised for robust growth in the coming decades, propelled by advancements in technology, increasing demand, and investment in manufacturing capacities.

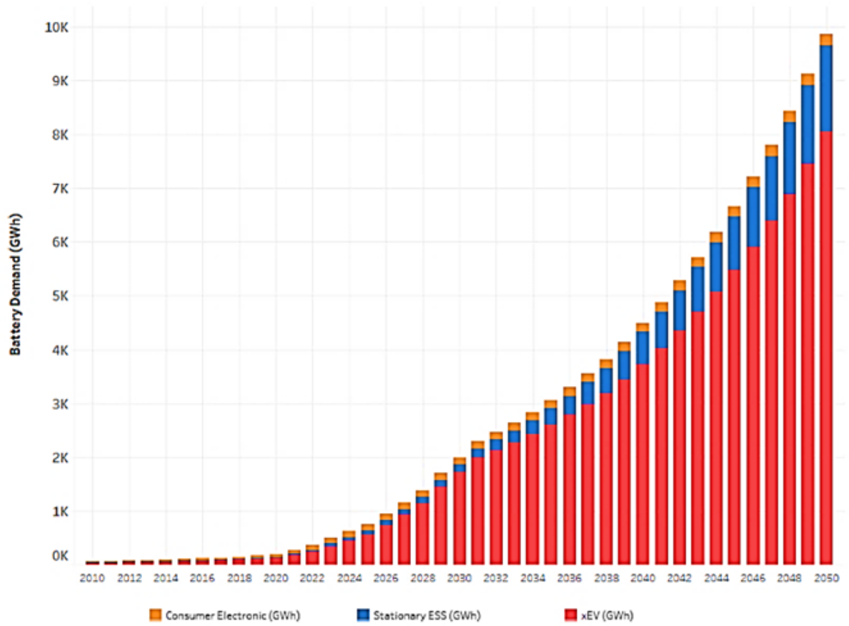

Figure 1.1 : Li-ion battery global market between 2010 and 2050 [5].

1.3 Mining Sites for Important Components in Lithium-Ion Batteries

Lithium, a critical component of LIBs, is produced primarily from two sources - brine and spodumene. The key countries that contribute to lithium production from brine are Chile and Argentina. On the other hand, Australia is the largest producer of lithium from spodumene, contributing 55,000 tonnes out of the 100,000 tonnes produced globally in 2021. China is also a significant contributor to lithium production.

The production of cobalt, another crucial element in LIBs, is highly concentrated in specific geographical locations. The Democratic Republic of Congo leads global cobalt production, contributing to 71% of the total, followed by Russia (4.5%), and Australia (3.3%). However, China, despite its modest share in cobalt mining, is a key player in cobalt refining and processing, with over 70% of global cobalt being refined there.

Nickel and manganese, while not as critical as lithium and cobalt, are still significant in the production of LIBs. As of the last data available in 2021, there was no significant supply risk for these elements, and their production locations are more geographically diverse.

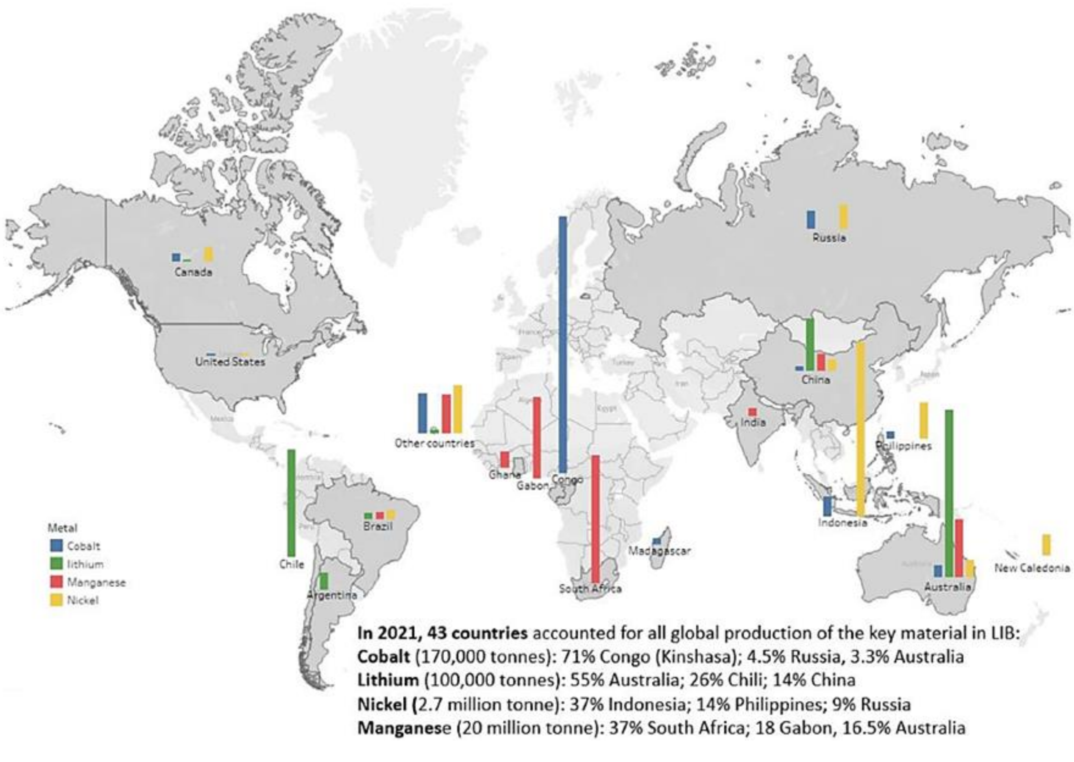

Figure 1.2 : Mining locations of the key elements used in Li-ion batteries [5].

In summary, the mining of key elements for LIB production is often concentrated in specific regions, posing potential supply risks due to geopolitical and environmental factors. For the sustainability of the growing LIB market, it is vital to address these risks and ensure a diversified and secure supply chain.

1.4 Production of Raw Materials for Lithium-Ion Batteries: 2020-2030

Lithium production has seen substantial growth over the years, driven by the increasing demand for LIBs. In 2020, the annual production of lithium was approximately 364,000 tonnes per year. Projections indicate that lithium production could escalate significantly to reach almost 1.59 million tones per year (measured in lithium carbonate equivalent) by the end of 2030.

Cobalt is another significant material in the manufacturing of LIBs. In 2020, the cobalt production stood at a noteworthy level, with expectations for this trend to continue. According to projections, the annual production of cobalt is likely to reach nearly 300,000 tons per year by 2030, primarily facilitated by new investments.

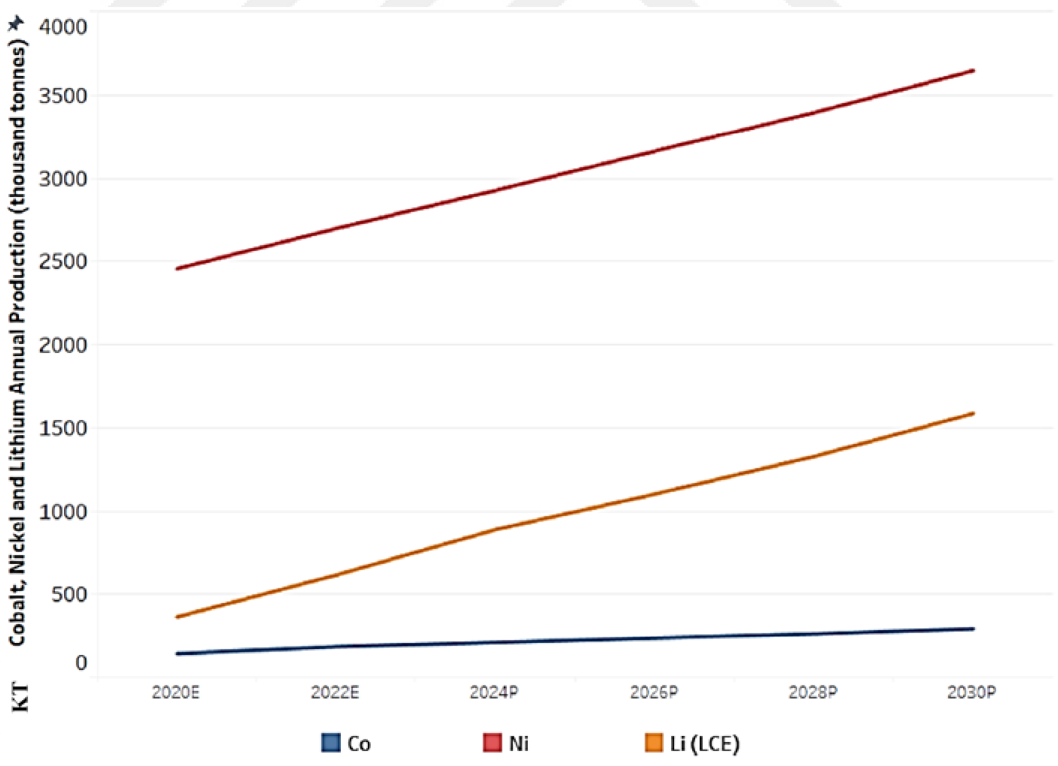

Figure 1.3 : Estimated raw material production between 2020 and 2030. Letter "E" indicates the estimated values, while the letter "P" indicates the projected values in the future [5].

Nickel, while not as critical as lithium and cobalt, is still an important material in the LIB production process. In 2020, the annual production of nickel was approximately 2.51 million tones. With the increasing demand for LIBs, the nickel production is estimated to increase further, reaching more than 3.65 million tones per year by 2030.

1.5 Overview of The Environmental Impacts of Waste Lithium-Ion Batteries

The environmental impacts of LIBs are multifaceted and can occur at various stages of the battery life cycle, including production, use, and disposal.

During production, the extraction of raw materials and manufacturing processes of LIBs can have significant environmental impacts. For example, the production of LIBs involves the mining of lithium, cobalt, and other metals, which can result in habitat destruction and water pollution. The mining of these materials can also contribute to air pollution through the release of dust and particulates. In addition, the production of LIBs requires large amounts of energy, which can result in greenhouse gas emissions if the energy is generated from fossil fuels.

The use of LIBs can also have environmental impacts. For example, the charging and discharging of LIBs can result in the release of greenhouse gases from the generation of electricity used to charge them. In addition, the transportation of LIBs for recycling or disposal can also contribute to greenhouse gas emissions. The use of LIBs in electric vehicles, in particular, has been shown to have lower greenhouse gas emissions compared to traditional gasoline-powered vehicles, but the overall environmental impact depends on the source of the electricity used to charge them [4].

The disposal of LIBs is a major environmental concern, as they can release hazardous substances such as cobalt and lithium into the environment if not properly managed. Landfills are not a suitable disposal option for LIBs due to the risk of leakage and the potential for hazardous substances to leach into soil and water. Incineration is also not a suitable option due to the release of harmful air pollutants [4].

Recycling of LIBs can help to mitigate the environmental impacts of their disposal, as it allows for the recovery of valuable materials for reuse and reduces the demand for the mining of new raw materials. However, the recycling of LIBs can also have environmental impacts, such as the release of harmful chemicals and greenhouse gases during the recycling process. It is important to adopt sustainable practices in the recycling of LIBs to minimize these impacts.

To mitigate the environmental impacts of LIBs, it is important to adopt sustainable practices throughout the battery life cycle. This can include sourcing raw materials responsibly, reducing energy consumption during production, and promoting the recycling of LIBs at the end of their life. Furthermore, the creation of cutting-edge recycling technologies can assist in minimizing the negative environmental effects of LIBs and recovering valuable materials for reuse.

Overall, the environmental impacts of LIBs are a complex issue that requires a multifaceted approach to address.

1.6 Overview of Current State of the Art in Metal Recovery from Waste Lithium-Ion Batteries

Lithium-ion Cobalt, nickel, manganese, and lithium are just a few of the priceless metals that are included within lithium-ion batteries. Once removed, these metals may be used again to create new batteries or a variety of products. Pyrometallurgical and hydrometallurgical methods have both been developed for the extraction of these metals from used lithium-ion batteries.

Smelting, a frequently used pyrometallurgical process, involves melting and segregating metals in a very hot furnace. This technique has the benefit of making it easier to recover a wide variety of metals from the batteries. Environmental issues might arise since it can also produce large amounts of slag and other waste byproducts. Direct melting, roasting, and leaching are further pyrometallurgical methods created for the extraction of metals from used lithium-ion batteries [5].

Hydrometallurgical processes, on the other hand, involve the use of aqueous solutions to extract and purify the metals from the batteries. These processes are generally more environmentally friendly than pyrometallurgical processes, but they may be limited in their ability to recover certain types of metals. Some of the most commonly used hydrometallurgical processes for the recovery of metals from waste lithium-ion batteries include solvent extraction, electrodeposition, and precipitation [5].

One of the key challenges in the recovery of metals from waste lithium-ion batteries is the need to maintain a high degree of purity in the recovered metals. This is particularly important for cobalt, nickel and manganese which are often used in the cathodes of lithium-ion batteries and requires a high level of purity in order to maintain its performance. Other challenges include the need to optimize the efficiency of the recovery processes, and to minimize the environmental impacts of the recycling operations.

The development of new, more effective techniques for recovering metals from spent lithium-ion batteries has been the subject of extensive research in recent years. This has included the development of novel pyrometallurgical and hydrometallurgical processes, as well as the use of advanced analytical techniques to characterize the recovered metals and optimize the recycling processes. There has also been increasing interest in the use of recycling technologies that can be integrated into the manufacturing process, in order to reduce the environmental impacts of battery production and disposal [6].

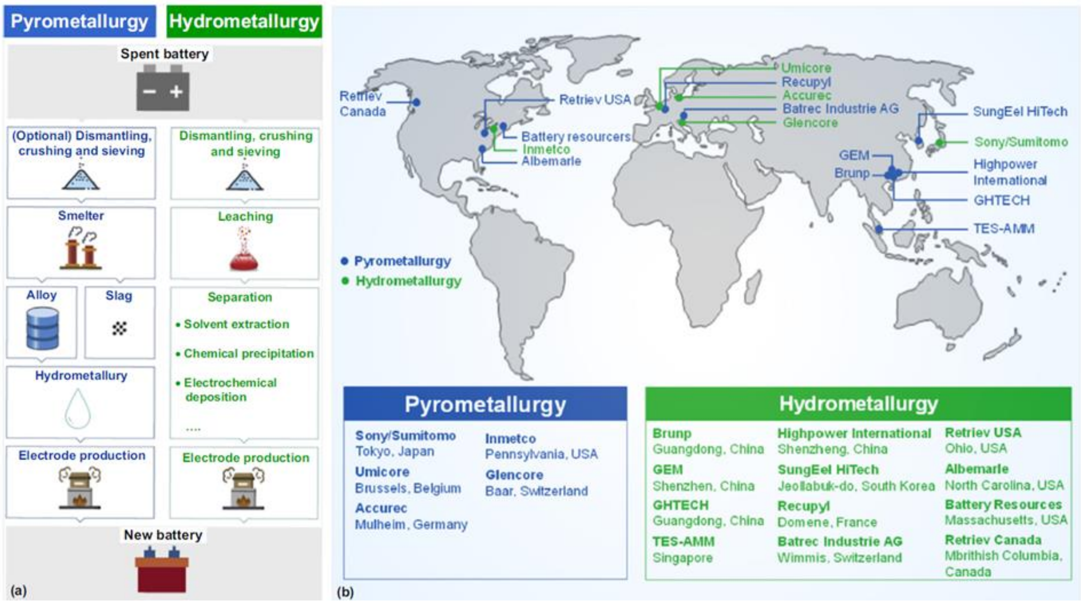

Figure 1.4 : (a) Pyrometallurgical and hydrometallurgical processes flow chart for spent LIB recycling processes. (b) Spent LIB recycling facilities worldwide [6].

The purpose of the present state of the art in metal recovery from used lithium-ion batteries is to increase the effectiveness and environmental sustainability of the recycling process, which is accomplished through a variety of methods and technologies that are being developed and evaluated. While there are still significant challenges to be addressed, the growing demand for portable electronic devices and the increasing awareness of the need for sustainable practices are likely to continue driving research and innovation in this field.

1.7 Objective and Focus of the Study: Metallurgical Routes for Metal Recovery

This thesis aims to investigate the potential of pyrometallurgical recycling as an effective and sustainable method for the recovery of valuable metals, specifically Cobalt, Nickel, Manganese and Copper from waste lithium-ion batteries.

The focus of this research will be on the use of pyrometallurgical recycling to recover Cobalt, Nickel, Manganese and Copper from waste lithium-ion batteries. These metals are particularly valuable and in-demand due to their use in the production of lithium-ion batteries, and their recovery from waste batteries could help to conserve resources and reduce the environmental impacts of mining.

In this research, a literature review will be conducted to thoroughly examine existing research on the use of pyrometallurgical recycling to recover valuable metals from lithium-ion batteries. This review will provide a foundation of knowledge on the advantages and limitations of this method, as well as the factors that can influence its performance. Based on the literature review, specific pyrometallurgical recycling processes will be designed and optimized for the recovery of valuable metals from waste lithium-ion batteries. This will involve identifying the optimal furnace temperatures and durations, as well as the use of any necessary additives. The performance of the developed pyrometallurgical recycling processes will then be evaluated by measuring and analyzing the recovery rates and purities of the recovered valuable metals. These results will be compared to those obtained using other metallurgical methods, such as hydrometallurgical recycling, to assess the relative performance of pyrometallurgical recycling. The environmental impacts of pyrometallurgical recycling will also be investigated by measuring and analyzing the greenhouse gas emissions and other pollutants generated during the process. Finally, based on the results of the research, recommendations will be made for the integration of pyrometallurgical recycling into the overall recycling process for lithium-ion batteries in a cost-effective and sustainable manner.

2. LITERATURE REVIEW

2.1 Overview of Lithium-Ion Battery Technology and Its Applications

Lithium-ion batteries, distinguishable by their high energy density and minimal self-discharge rate, represent a specific type of rechargeable battery that has seen a surge in popularity in recent times. As per a MarketsandMarkets report, the lithium-ion battery market is projected to experience robust growth, expanding from USD 42.7 billion in 2020 to an estimated USD 93.1 billion by 2025. This progression corresponds to a compound annual growth rate (CAGR) of 17.4% throughout the forecast duration.

The fundamental mechanism of lithium-ion battery technology revolves around the transfer of lithium ions between the cathode and anode during the cycles of charge and discharge. A lithium-ion battery typically consists of a graphite anode, while the cathode is composed of lithium-containing materials such as lithium cobalt oxide ($LiCoO_2$) or lithium iron phosphate ($LiFePO_4$). Generally, the electrolyte is formed by dissolving a lithium salt in an organic solvent, facilitating the migration of ions between the anode and cathode [7].

These batteries find application in a multitude of products, including but not limited to, portable electronics, electric vehicles, and renewable energy storage systems. Their high energy density, coupled with their capacity to encapsulate substantial amounts of energy in a relatively compact and lightweight form, renders them particularly appropriate for use in electric vehicles. Moreover, their low self-discharge rate enables them to retain most of their charge over extended periods of non-utilization [8].

The production of lithium-ion batteries generates a significant amount of waste, in the form of discarded batteries, as well as manufacturing scraps and process materials. These materials contain valuable metals such as lithium, cobalt, nickel, and other metals which can be recovered by metallurgical routes [9].

A current topic of study focuses on closing material cycles, lowering dependency on new resources, and potential economic and environmental benefits of recovering valuable metals from used lithium-ion batteries through metallurgical processes. These processes mainly includes Pyro-metallurgical, Hydrometallurgical and Bio-metallurgical routes and their results show that these routes are highly effective in recovering metals from waste lithium-ion batteries with high recovery rates and low environmental impact. This thesis work on "Recovery of valuable metals from waste lithium-ion batteries by metallurgical routes" will focus on the experimentation and analysis of these metallurgical routes of recovery and extraction, including the evaluation of their efficiency, yield, environmental impact and scalability [10].

2.1.1 The undamental LIB principle and its construction

According to the definition given, a lithium-ion battery (LIB) is an electrochemical cell that produces energy through electrochemical reactions. The cathode, anode, electrolyte, separator, and current collector are the major parts of a LIB, as shown in Figure 2.1. When a lithium-ion battery is operating, electrical energy is transferred more easily thanks to the electrolyte-driven flow of lithium ions between the positive and negative electrodes. Graphite is used as the cathode and lithium-containing substances like $LiCoO_2$ or $LiFePO_4$ are used as the anode in the lithium-ion battery technology[11]. A single cell lithium-ion battery can be charged using just two stages (constant current and constant voltage), as opposed to the multiple steps required to charge multi-cell lithium-ion batteries (constant current, balance, and constant voltage)[12].Lithium-ion batteries also have the capacity to switch the cathode and anode's half-reactions:

$$LiCoO_2 \leftrightarrow Li_{1-x}CoO_2 + xLi^+ + xe- \text{ (cathodic half)} \tag{2.1}$$

$$xLi^+ + xe^- + 6C \leftrightarrow Li_xC_6 \text{ (anodic half)} \tag{2.2}$$

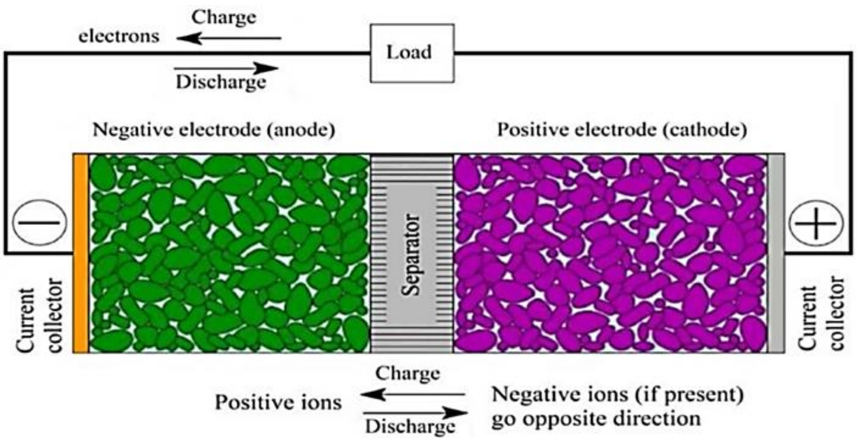

Figure 2.1 : The mere components of a LIB, as described in [93] are displayed.

When it comes to preventing short circuits and maintaining a safe distance between the anode and cathode during charging and discharging, the separator in a lithium-ion battery is essential [13]. It does this by enabling ions to pass through a porous, thin membrane. Additionally, according to [14], aluminum is frequently utilized on the battery's cathode side, but copper is frequently employed on the anode side as a current collector. To allow for the flow of electrical energy generated by the battery to various external devices such as cars, mobile phones, computers, cameras, and more, during the discharge phase, these current collectors are conductive materials that connect with each of the electrodes. Lithium-ion batteries hold a substantial advantage over other types of batteries, such as nickel-metal hydride (Ni-MH), nickel-cadmium (Ni-Cd), lead-acid, lithium metal, and phosphorous-lithium (PLion) batteries. This is largely due to their notable characteristics including a higher energy density, extended lifespan, and minimal memory effect. These attributes underscore the extensive adoption of lithium-ion batteries across a wide range of applications.

2.1.2 Anode materials

According to [15], the anode is a crucial and effective component in lithium-ion batteries. It plays a significant role in the battery's function and performance because it is responsible for absorbing lithium ions during the charging process. Contemporary lithium-ion batteries often employ a diverse array of materials for anode construction, including lithium, silicon, graphite, and intermetallic or lithium-alloying compounds. These anode materials typically exhibit critical chemical and physical properties that contribute to energy storage and are influenced by factors such as size, shape, and modifications. Studies have indicated that the utilization of anode materials in the nanoscale size range can enhance the electrochemical performance of lithium-ion batteries [16]. Figure 2.2 displays the potential voltage and capacity of several anode materials, including titanium oxides, MO_x, MP_x, MN_x, MS_x, Si, Ge, Al, Sn, Sb, and porous carbon. Furthermore, Table 2.1 elucidates the advantages and disadvantages associated with various types of anode materials.

2.1.3 Cathode materials

As articulated in [17], the cathode – synonymous with the positive electrode – constitutes a critical part of a lithium-ion battery's architecture. The constituent material and the inherent characteristics of the cathode directly impact the operational efficiency of the battery. This is principally because the cathode's primary role during the discharge phase is to assimilate lithium ions, a process that ultimately determines the energy output and capacity of the battery. Instead, active substances containing lithium ions, such as lithium oxide, are commonly employed. To enhance conductivity and create a bonding between active components and additives on the aluminum layer, additives and binders are often added. According to [18], the presence of a significant amount of lithium has a significant impact on a battery's capacity, voltage, and potential difference. Lithium metal oxides include substances like $LiCoO_2$, $LiMn_2O_4$, and $Li(Ni_xMn_yCo_z)O_2$. Lithium-ion batteries can use a variety of rechargeable cathode materials, including olivines ($LiFePO_4$), vanadium oxide, and lithium oxide. $Li(Ni_xMn_yCo_z)O_2$, commonly known as NMC, can replace $LiCoO_2$ and has a reduced failure rate, although $LiCoO_2$ has a higher reactivity and is used as an oxygen source. These cathode materials have an energy density of 600 Wh/kg and a capacity range of roughly 120-160Ah/kg, while the energy density is reduced to 100 Wh/kg when packaged in practical devices. There are advantages and disadvantages to using various cathode materials, such as those based on manganese and cobalt, including cycle instability and high cost. In the sphere of cathode materials for lithium-ion batteries, certain alternatives to Lithium Nickel Manganese Cobalt Oxide (NMC) are gaining traction. One such alternative is the Lithium-Manganese rich transition metal oxide, which, while bearing similarities to NMC, exhibits a greater concentration of manganese and lithium [19]. Another increasingly favored cathode material is Lithium Iron Phosphate ($LiFePO_4$). $LiFePO_4$ stands out due to its superior safety measures, impressive cycle performance, stable voltage profile, and economic feasibility. Owing to these attributes, LiFePO4 batteries have found substantial applications in automotive and other industries, presenting a safer substitute to Lithium Nickel Cobalt Aluminum Oxide ($LiNiCoAlO_2$) batteries [20]. However, this by no means diminishes the importance of our focus on NMC, which continues to remain a pivotal area of our research.

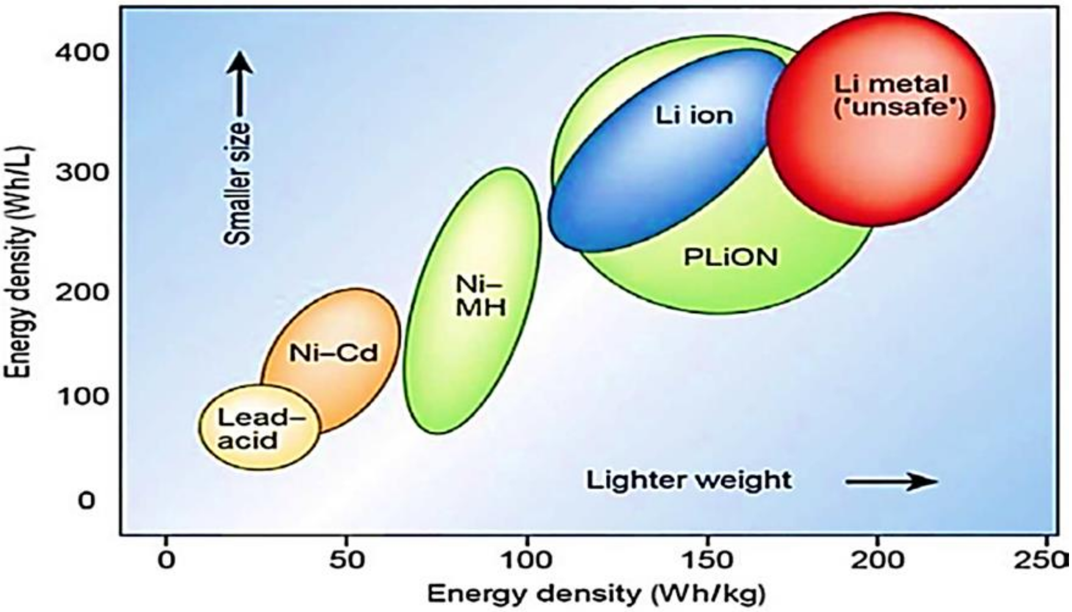

Figure 2.2 : Comparison of Specific Energy and Energy Densities across Various Types of Rechargeable Batteries [20].

2.1.4 Electrolyte

An electrolyte is a material that serves as a medium for ion transfer in lithium-ion batteries, as was previously mentioned in [21]. The optimal electrolyte should have a number of essential qualities, including strong ionic conductivity, thermal stability, nontoxicity, and electrochemical stability. These qualities can be obtained by combining several kinds of lithium salts, such as $LiPF_6$, $LiAsF_6$, and $LiClO_4$ with organic carbonates, such as carbonate or diethyl carbonate, ethyl methyl carbonate [22]. A solid, a liquid, or any mix of the two can be an electrolyte. Liquid electrolytes and polymer-based electrolytes are the two types of electrolytes most frequently used in rechargeable lithium-ion batteries. These latter ones are renowned for having conductive properties that make it possible to combine them with ceramic nanoparticles to produce composites with great voltage resistance. They reduce the likelihood of lithium dendrite formation and have a higher viscosity, making them appropriate for use with lithium metal anodes. The polymer used to make the electrolyte often determines the conductivity characteristics of polymer-based electrolytes. The poor ion conductivity of these electrolytes, however, can be a serious issue. By choosing a liquid electrolyte with a variety of solvents and suitable dielectric and viscosity characteristics, one can get around this barrier and enable a high rate of ion conduction. Optimizing the dielectric and viscosity constants in the ion conduction system is how the field-trials procedure is carried out for liquid electrolytes [23]. The various kinds of typical salts and solvents used in lithium-ion battery electrolytes are displayed in Tables 2.1 and 2.2.

2.1.5 Separator

According to the insights presented in [24], the separator in a lithium-ion battery serves a dual purpose, both of which are integral to the battery's safe and effective functioning. Primarily, it functions as a protective partition between the anode and the cathode electrodes, mitigating the risk of potential short-circuits. Concurrently, it contributes to the thermal stability of the battery by preserving an optimal distance between the two electrodes, thereby preventing thermal runaway. The structure and behavior of the separator has a significant impact on a number of lithium-ion battery performance metrics, including energy density, battery safety, power density, cycle life, and others. The separator does not appear to undergo any chemical reaction, yet ion transport during charging and discharging is made possible by its porous structure. To avoid thermal runaway during short circuit events, the separator ought to have a blocking interface function [25,26]. Based on their physical and chemical characteristics, separators in lithium-ion batteries can be categorized as woven, molded, nonwoven, bonded, microporous, paper-based, or laminated varieties. At the moment, separators for lithium-ion batteries are created using microporous polymeric films or nonwoven textiles. Typically, no separator is needed for batteries that use polymer-based or solid-state electrolytes. The majority of the time, however, microporous type separators made of polyolefin (PE, PP, PP/PE/PP) are used in lithium-ion battery systems with liquid electrolytes [27].

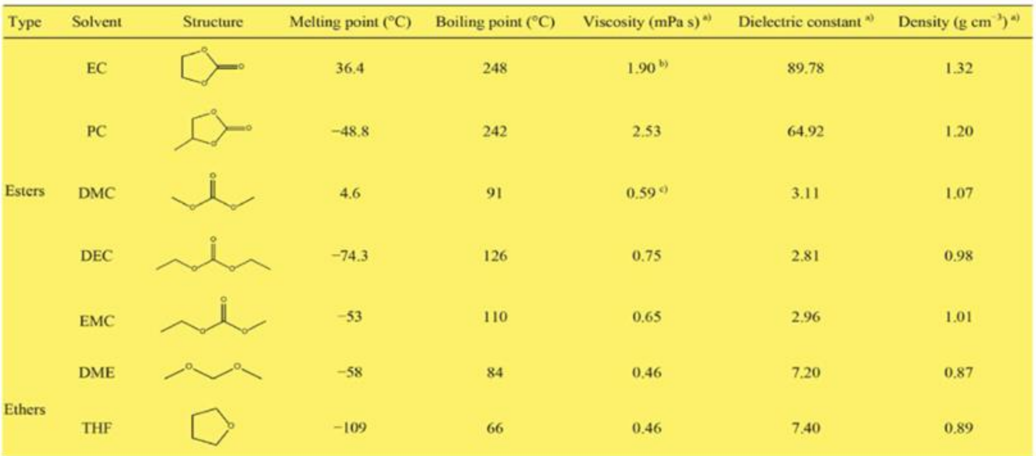

Type	Solvent	Structure	Melting point (°C)	Boiling point (°C)	Viscosity (mPa s) [a]	Dielectric constant [a]	Density (g cm^{-3}) [a]
Esters	EC		36.4	248	1.90 [b]	89.78	1.32
	PC		−48.8	242	2.53	64.92	1.20
	DMC		4.6	91	0.59 [c]	3.11	1.07
	DEC		−74.3	126	0.75	2.81	0.98
	EMC		−53	110	0.65	2.96	1.01
Ethers	DME		−58	84	0.46	7.20	0.87
	THF		−109	66	0.46	7.40	0.89

Figure 2.3 : Exhibition of common solvents in electrolyte of LIBs [29,30].

Table 2.1 : Merits and demerits for several anode materials [28].

Material	Mertis	Demerita
Alloys	Great specific capacity (400-2300 $mAhg^{-1}$) Enough safety Nice cycle life Satisfactory columbic efficiency	Lower conductivity Much volume change Capacity loss
Silicon	Improved capacity range (3579 $mAhg^{-1}$) Desolated	Unexpected volume change (300%)
Carbon	Cheap` Better safety Great structure High Conductivity feature Long life Available and low cost	Capacity limitation Safety irregularities Long life Lessen discharge rate
Transition metal oxides	Tremendous specific capacity (600-1000 $mAhg^{-1}$) Enough stability	Poor Columbic Efficiency Max potential hysteresis

Table 2.2 : Exhibition of common salts in electrolyte of LIBs [29].

Salts	$LiClO_4$	$LiPF_6$	$LiAsF_6$	$LiN(SO_2CF_3)_2$	$LiBF_4$	$LiN(SO_2F)_2$
Al corrosion*a	N	N	N	Y	N	Y
H_2O sensitivity*a	N	Y	Y	Y	Y	Y
Ionic consuxtivity (mS) cm^{-1} *b	9.0	10.0	11.1*c	6.2	4.5	10.4*c

*a. Y and N represents yes and no, respectively; the ionic conductivity of 1 mol L^{-1} salt dissolved in EC/DMC at *b. 20 ◦C, and *c. 25 ◦C.

2.2 Characterization of Waste Lithium-Ion Batteries and Assessment of Their Metal Content

The process of characterizing waste lithium-ion batteries and evaluating their metal content is paramount in the metallurgical extraction of valuable metals contained within these power sources. Characterization entails a comprehensive analysis, focusing on aspects such as the batteries' chemical composition, physical properties, and microstructural attributes. Meanwhile, the metal content assessment is a quantitative operation aimed at identifying and enumerating the disparate metals incorporated in the batteries, along with detailing their distribution across the various components within the battery structure.

The fundamental components of a lithium-ion battery encompass the anode, cathode, and the electrolyte. Predominantly, the cathode is fabricated from lithium cobalt oxide ($LiCoO_2$), lithium manganese oxide ($LiMn_2O_4$), or lithium iron phosphate ($LiFePO_4$), while the anode is typically composed of graphite. The electrolyte usually involves a lithium salt suspended in an organic solvent. Disposed lithium-ion batteries consist of the aforementioned anode, cathode, and electrolyte, in addition to minor components such as the separator and current collector.

To characterize the constituents of spent lithium-ion batteries, various analytical techniques are employed, which include X-ray diffraction (XRD), scanning electron microscopy (SEM), energy-dispersive X-ray spectroscopy (EDS), and inductively coupled plasma mass spectrometry (ICP-MS). These methodologies facilitate an assessment of the batteries' metal content, unveiling their chemical composition, physical properties, and microstructural elements.

In our research, we have exploited the benefits of these techniques, with specific focus on ICP, XRD, and X-ray Fluorescence (XRF), to deliver in-depth analysis of our samples, both before and after experimental procedures. The crystal structure of the metals found in batteries can be ascertained using XRD, while images of the surface morphology can be obtained using SEM, and the elemental makeup of the batteries can be ascertained using EDS. On the other hand, the concentration of different metals present in the batteries can be quantitatively determined using ICP-MS.

The characterization of used lithium-ion batteries and evaluation of their metal contents have been the subject of numerous research projects. For instance, Liu et alwork .'s from 2018 described how they used XRD, SEM, and EDS to characterize used lithium-ion batteries. Cobalt, nickel, and lithium were revealed to be the key metals in the batteries, according to the study. In a different study, [31] it was stated that the metal content of used lithium-ion batteries was determined using ICP-MS. According to the study, cobalt, nickel, and lithium were the key metals identified in batteries, along with minor elements including manganese and iron.

The research delineated in [32] employed X-ray Diffraction (XRD) and Scanning Electron Microscopy (SEM) to systematically characterize the microstructures of waste lithium-ion batteries. The investigation revealed distinctive differences between the microstructures of the anode and cathode in these batteries. More specifically, the primary constituent of the anode was found to be graphite, while the cathode was predominantly composed of lithium cobalt oxide. Furthermore, the study uncovered that the batteries' metal content was primarily dominated by cobalt, nickel, and lithium. In [33] they reported on a study that used ICP-MS to quantitatively determine the concentration of various metals present in waste lithium-ion batteries. The study found that the main metals present in the batteries were cobalt, nickel, and lithium, with small amounts of other metals such as manganese, iron, and aluminum also present.

In summary, characterization of waste lithium-ion batteries and assessment of their metal content is an essential step in the recovery of valuable metals from these batteries using metallurgical routes. The use of appropriate analytical techniques can provide information on the chemical composition, physical properties, and microstructural features of the batteries, which can be used to identify the main metals present and to optimize the recovery process.

2.2.1 LIB cathode material and main types

Since they have a high energy density, a long lifespan, quick charging capabilities, the capacity to work in a variety of temperatures, no memory effect, and are non-polluting, LIBs have become widely used in electronic gadgets and electric vehicles during the past 10 years. The many LIB kinds are typically divided into four categories.

2.2.2 Lithium Cobalt Oxide (LCO)

The lithium cobalt oxide ($LiCoO_2$) battery is a layered inorganic compound and its chemical formula is $LiCoO_2$. When compared to other LIBs, LCO batteries are determined to have the highest theoretical energy density and volume specific energy, according to the literature [34]. A constant operating voltage, superior cycle stability, and a high compaction density are further advantages of LCO batteries [35]. The operational voltage of LCO batteries has increased from 4.2 V to 4.45 V as a result of growing consumer demand for them and related research. The practical specific capacity of LCO has gotten to 185 mAh/g and is getting close to its 274 mAh/g theoretical specific capacity [36]. The majority of 3C electronic devices use LCO batteries. Li-ion is detached while charging, which causes LCO electrode reactions:

$$LiCoO_2 \rightarrow Li_{1-x}CoO_2 + {}_{x}Li^{+} + xe^{-} \quad (2.3)$$

During the discharging process: Li-ion is embedded:

$$Li_{1-x}CoO2 + {}_{x}Li^{+} + {}_{x}e^{-} \rightarrow LiCoO_2 \quad (2.4)$$

The lithium cobalt oxide ($LiCoO_2$) or LCO has a spinel structure as well as a layered structure. The latter is known to have better chemical properties. The process of charge-discharge involves continuous detachment and embedding of Li ions between

CoO_2 layers and it is through this process that LCO is able to maintain the layered structure stable without collapse as depicted in Figure 2.3 [37]. The capacity of the LCO battery will, however, steadily decline as the charge-discharge cycle continues. This is mostly attributable to crystal flaws caused by the continual expansion and contraction of the lithium cobaltate crystal structure during the charge-discharge process. The altered crystal structure that results from this mechanism also causes grain collapse and fracture [38]. In the conclusion, this leads to a reduction in the cathode material, an increase in internal resistance, and a reduction in specific capacity phase purity, crystallinity, and orientation of the cathode thin films that are critical factors in thin-film battery development, according to [39].

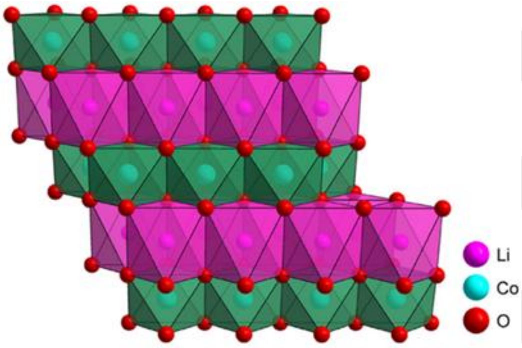

Figure 2.4 : Crystalline structure of layered $LiCoO_2$ [37].

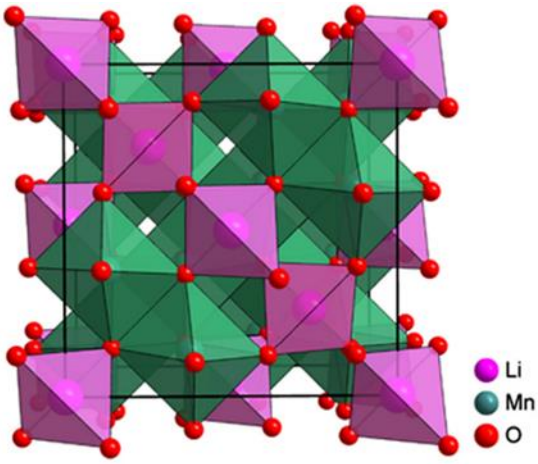

Figure 2.5 : Crystalline structure of spinel $LiMn_2O$ [37].

2.2.3 Lithium Manganate Oxide (LMO)

The cathode of a Lithium manganese oxide ($LiMn_2O4$) or LMO battery is constructed from $LiMn_2O_4$, exhibiting a cubic spinel crystal structure, illustrated in Figure 2.4 [37]. At the atomic level, a single LMO cell is made up of 56 atoms, encompassing 8 lithium atoms, 16 manganese atoms, and 32 oxygen atoms. The lithium ions, depicted in green, have the capacity to freely traverse the lattice structure via a process of extraction and insertion throughout the charge-discharge cycle.

The electrochemical reactions occurring in the LMO electrodes can be articulated as follows: During the charge cycle, the Li-ion is extricated:

$$LiMn_2O_4 \rightarrow LixMn_2O_4 + (1 - x)Li^+ + (1 - x)e^- \tag{2.5}$$

During the discharging process, Li-ion is embedded:

$$LixMn_2O_4 + (1 - x)Li^+ + (1 - x)e^- \rightarrow LiMn_2O_4 \tag{2.6}$$

The electrochemical reaction of LMO (Lithium Manganese Oxide) is stated to occur between a voltage range of 3.0 to 4.5 V, and its theoretical specific capacity is calculated to be 148 mAh/g [40].

Lithium Manganese Oxide (LMO) batteries present several benefits, among which their superior electrochemical performance, abundant reserves, and environmentally friendly nature stand out. However, practical applications of LMO batteries have revealed some deficiencies, such as accelerated capacity decay, a relatively low specific capacity, subpar conductivity, inefficient ion diffusion, and pronounced structural alterations ensuing a charge-discharge cycle. As highlighted in [41], these limitations in the materials currently employed in energy storage systems and electric vehicles have spurred researchers to explore alternative solutions. A promising proposal, as delineated by Wujie Dong et al. in [42], involves the formation of a 2-3 nm artificial solid electrolyte interphase (SEI) layer. This innovation has shown potential in meeting high standards of energy density, longevity, safety, cost-effectiveness, as well as rapid charge and discharge capabilities.

2.2.4 Lithium Iron Phosphate (LFP)

As depicted in Figure 2.5, the cathode of a Lithium Iron Phosphate ($LiFePO_4$) or LFP battery consists of the chemical compound $LiFePO_4$, which manifests an archetypal olivine crystal structure [43]. Each cell within the LFP battery contains four LFP units. In such an arrangement, the oxygen atoms are assembled in quasi-hexagonal patterns. Lithium ions within LFP are conferred two-dimensional mobility, permitting free movement during the charge-discharge cycle, courtesy of this structural configuration. A fundamental attribute of LFP lies in the exceptional stability of its PO4 3- polymeric tetrahedron. LFP batteries are further distinguished by their prolonged charge-discharge curve plateau and their enhanced security in high-temperature conditions. Consequently, among lithium batteries, the LFP battery holds the highest safety standard.

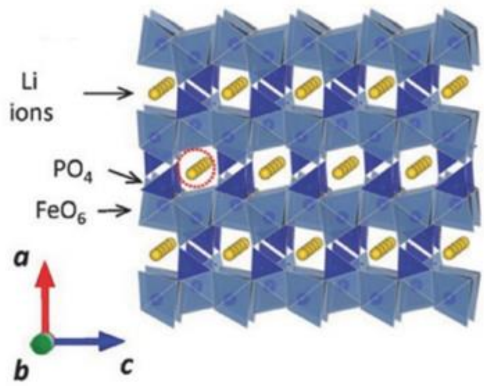

Figure 2.6 : Crystal structure of LFP cathode [43].

The reactions of LFP electrodes are as follows:

During the charging process, Li-ion is detached:

$$LiFePO_4 - xLi^+ - xe^- \rightarrow xFePO_4 + (1 - x)LiFePO_4 \tag{2.7}$$

During the discharging process: Li-ion is embedded:

$$FePO_4 + xLi^+ + xe^- \rightarrow xLiFePO_4 + (1 - x)LiFePO_4 \tag{2.8}$$

In theory, the LFP (Lithium Iron Phosphate) cathode material possesses an electrochemical specific capacity of 170 mAh/g. The potential of the lithium metal electrode approximates to 3.45 V, and it has a theoretical energy density of 550 wh/kg. Yet, due to the limited conductivity of LFP, the actual discharge capacity reduces to 113 mAh/g, with only 0.6 mol of lithium ion being utilized for the intercalation and deintercalation cycle at ambient temperature. Despite this, LFP batteries have been demonstrated to possess commendable cycle performance. A 6.81% reduction in lithium ion volume upon deintercalation [44] compensates for the carbon anode's volume shift during discharge, thereby extending the LFP battery's cycle lifespan. Owing to their high specific energy, consistent charge and discharge platform, elevated safety, long cycle life, and cost-effectiveness, LFP batteries find extensive use in electric vehicle power batteries and energy storage systems [45]. Researchers have validated the application of thermally modulated LFP batteries, which provide an adequate cruising range per charge that can be extended by a 10-minute recharge in all weather conditions [46]. Furthermore, LFP is frequently adopted in auxiliary transport vehicles in deep coal mines due to its superior safety performance.

2.2.5 Lithium Nickel Manganese Cobalt Oxides (NCM)

The cathode material in NCM batteries typically comprises a composite of three chemical elements: nickel, cobalt, and manganese, as indicated by the $LiNi_xCo_yMn_zO_2$ chemical formula. As illustrated in Figure 2.6, this formula sustains the layered - $NaFeO_2$ structure, which incorporates transition elements and lithium elements in every layer. According to [47], this crystal structure can be conceptualized as the sequential accumulation of the transition metal layer, oxygen layer, lithium layer, and a subsequent oxygen layer.

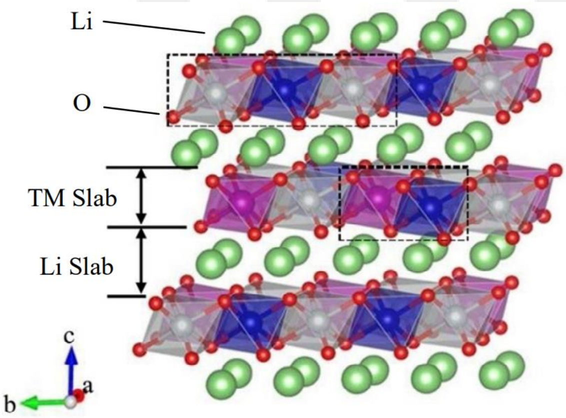

Figure 2.7 : Representation of NCM Cathode's Crystal Structure: Distinguishing Ni, Co, and Mn Atoms in the Transition Metal (TM) Layer as Depicted by Gray, Blue, and Purple Spheres Respectively, with Red Spheres Indicating O Atoms [47].

The normal composition ratio of nickel cobalt manganese (NCM) material is 111, 523, and 811, respectively, indicating the concentration of nickel, cobalt, and manganese, according to the literature [48,49]. The specific energy of an NCM battery rises as the fraction of nickel in the material increases, and the performance stability of the battery increases as the proportion of cobalt rises. Additionally, a higher manganese concentration raises the battery's output voltage.

NCM material, which has a theoretical capacity of 278 mAh/g, is distinguished by its excellent comprehensive performance as a result of its special mix of the features of nickel, cobalt, and manganese.

Another cathode material created in tandem with NCM is nickel cobalt aluminum (NCA), which shares the same layered structure as NCM and NaFeO2. However, NCA has a little lower working voltage than NCM due to the absence of manganese components. When nickel, cobalt, and aluminum are distributed in the ratio of 0.8:0.15:0.05, the best electrochemical performance is noted [50]. Although NCA material performs similarly to NCM, its market share is still quite modest.

Large-sized nickel-cobalt-manganese ternary composite oxide agglomerate microspheres were explored in [51], who found that lowering the material's specific surface area can lower the frequency of unfavorable interfacial side reactions.

The NCM material, constituting 67.37% of lithium batteries in electric vehicles, is noted for its high specific energy, long life cycle, steady discharge, and robust low-temperature performance. However, relative to LFP batteries, it carries a heightened safety risk, potentially leading to a domino effect post a single battery thermal runaway, culminating in a fire and battery pack explosion. Consequently, its application in subterranean coal mines is presently proscribed.

3. METHODS FOR RECOVERING VALUABLE METALS FROM WASTE LITHIUM-ION BATTERIES

The recovery of valuable metals from waste lithium-ion batteries has been the subject of much research in recent years. A number of methods have been developed to recover these metals, including pyrometallurgical, hydrometallurgical, mechanical, and biometallurgical techniques.

Pyrometallurgical techniques, such as smelting and refining, involve high temperature processes to extract valuable metals from waste lithium-ion batteries. These methods have been found to be effective in recovering copper and aluminum, as well as lithium, cobalt, and nickel [52]. However, pyrometallurgical techniques also produce emissions that can be harmful to the environment and require significant energy inputs.

Hydrometallurgical techniques, on the other hand, use liquids and chemicals to extract valuable metals from waste lithium-ion batteries. These techniques include leaching, solvent extraction, and electrowinning, which have been found to be effective in recovering a wide range of metals, including cobalt and nickel [52]. However, these methods can also produce waste streams that are difficult to manage, and require chemicals that can be harmful to the environment.

Mechanical recycling techniques use physical processes to separate and recover valuable metals from waste lithium-ion batteries. These techniques include shredding, sorting, and grinding, which have been found to be effective in recovering metals such as copper and aluminum [53]. However, these methods are labor-intensive, and can also produce emissions that are harmful to the environment.

Finally, biometallurgical techniques use microorganisms or enzymes to extract valuable metals from waste lithium-ion batteries. These techniques include bioleaching and biosorption, which have been found to be effective in recovering metals such as copper and nickel [54]. However, these methods are still in the early stages of development, and more research is needed to understand their full potential.

In conclusion, there are a variety of methods for recovering valuable metals from waste lithium-ion batteries, each with its own advantages and disadvantages. In the following sections of this chapter, we will provide a detailed discussion on each of these existing methods.

The improper disposal of electrolyte from spent lithium-ion batteries (LIBs) can result in severe safety and environmental hazards, due to the highly soluble nature of these substances in water [4]. At the same time, the electrolyte has a high potential value as a resource that can be recovered. The proper recovery of electrolyte is therefore a challenge worthy of further research and study.

Several nations have started enacting regulations for the recycling of old batteries in an effort to increase the safety, effectiveness, and sustainability of the battery business and lessen the detrimental effects of spent batteries on society and the environment. These rules specify who and what is in charge of collecting and discarding used rechargeable batteries, including battery producers, nearby merchants, and end-users.

As depicted in Figure 3.1, various methods for recycling end-of-life (EoL) Lithium-Ion Batteries (LIBs) exist, each accompanied by distinct benefits. The two primary recycling techniques for EoL LIBs are pyrometallurgical and hydrometallurgical methods, as indicated by references [23,24]. Another approach is direct recycling, albeit its usage is confined to specialized applications, representing less than 5% of the total recycling market, as per [25,26]; hence, this technique is not emphasized in Figure 3.1.

The pyrometallurgical method involves the reduction of component metal oxides into an alloy of Co, Cu, Fe, and Ni in a high-temperature furnace, as described in [24]. However, this approach is not optimal, yielding recovered materials in a range of 50-85%, as cited in [27,28]. On the contrary, preprocessing or pretreating LIBs leads to a significantly higher recovery yield, exceeding 90%, according to [27,28].

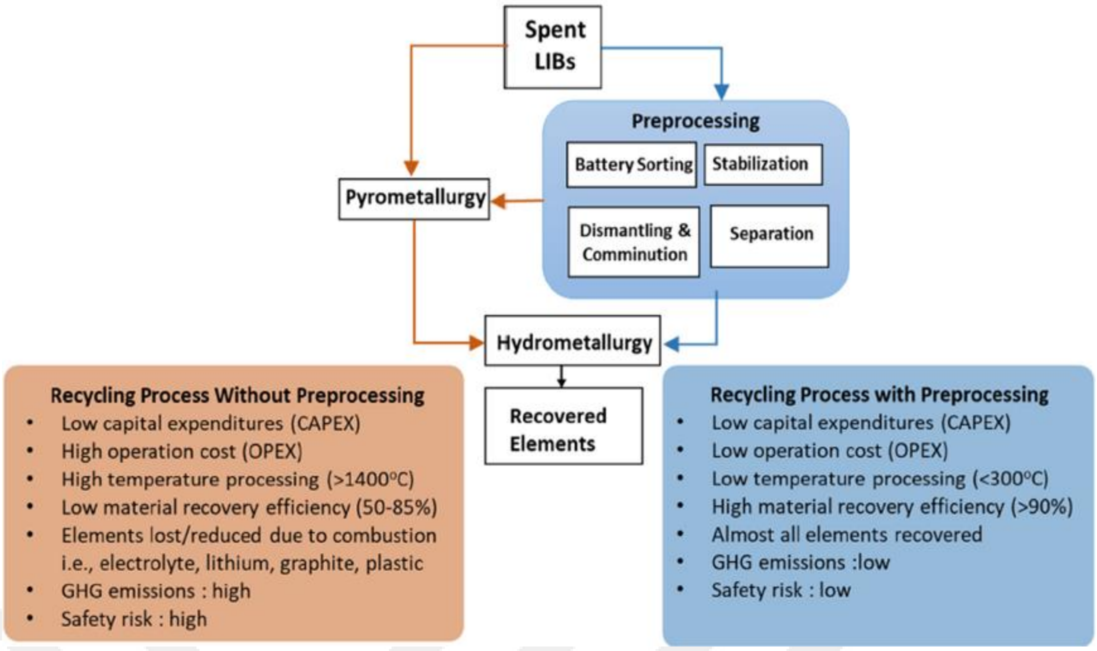

Figure 3.1 : Comparison of LIB recycling processes with and without preprocessing.

3.1 Battery Sorting

Battery sorting is crucial not only to remove non-battery waste but also to categorize batteries based on chemistry, dimensions, health, and further recycling requirements [55]. Manual and automated approaches exist, with multistage sorting enhancing efficiency [56,57].

3.1.1 Physical appearance-based sorting

Initially, waste is moved by conveyors for presorting, with large trash items manually removed [58]. Remaining batteries undergo magnetic sorting followed by mechanical separation. Shaker screens sort the batteries by size and shape at high speed [59]. Though often done manually, machine learning and X-ray techniques are explored for sorting spent LIBs [60,61].

3.1.2 Electrical parameters-based sorting

Simple sorting involves direct measurement of static (open state) and dynamic (energy flow state) parameters such as voltage, internal resistance, discharge capacity, and self-discharge rate [45,62]. Some dynamic parameters are difficult to measure without battery damage, hence, alternate methods such as CT and X-ray scanning are utilized, though they're not yet fully matured [56].

3.1.3 Machine learning model-based sorting

Sorting accuracy can be improved by using battery equivalent circuit models and machine learning algorithms, using parameters like voltage, current, and internal resistance [56]. This synergizes with the proliferation of big data and cloud storage, accelerating sorting [45,63].

3.1.4 Chemistry material-based sorting

Many recyclers sort batteries based on their chemistry or cathode material type (e.g., $LiCoO_2$ and $LiFePO_4$) to optimize hydrometallurgical processes. This involves identification of operating and electrochemical parameters [45,64]. However, due to challenges in identifying internal processes and lack of identifiable information on batteries, machine learning and deep learning models are being explored for identifying electrochemical parameters [65,66].

Many of these sorting techniques can also be leveraged for second life applications of batteries.

3.2 Stabilization

Lithium-ion batteries (LIBs) require stabilization prior to disassembly to prevent thermal runaway and the subsequent loss of valuable components and creation of hazardous substances [39,67]. Four primary stabilization methods are generally recognized:

3.2.1 Electrical discharge

Discharging LIBs is vital before dismantling to decrease self-ignition risks and short circuits. This is accomplished through several means:

a) Discharge via Metal Powder: LIBs are usually discharged first using a resistor, or through alternative methods employing graphite or metal chips. However, rapid discharge can lead to heat generation and possible explosions, especially for larger batteries [71,73].

b) Discharge via Electronic Load: Conventional load banks waste energy as heat when discharging spent LIBs. In contrast, modern regenerative electronic banks, coupled with converters, can recover 80–94.5% of the energy as alternating current. This method has limitations including additional sorting steps and reduced efficiency for severely drained batteries [75,76].

c) Discharge via Aqueous Solutions: In this method, the battery's electrodes are immersed in conductive solutions like salt, acid, or alkali causing a short circuit. Despite its safety, this approach can lead to solution contamination and release of hazardous compounds due to chemical reactions [77,78].

d) Discharge via Inductive Effect: Inspired by the inductive charging methods of smartphones, this novel approach uses inductive discharge. Still in the early stages of development, it demands more extensive research for broader implementation [75,82].

3.2.2 Thermal deactivation

Industrial processes and ongoing R&D have identified thermal deactivation as an effective way to fully deactivate LIBs, thereby preventing unexpected thermal events.

a) Cryogenic Deactivation: This method involves freezing the electrolyte in spent LIBs to cryogenic temperatures, thereby rendering them non-conductive. Despite its high costs, it is promising for processing large quantities of spent LIBs [84,85].

b) Heat Deactivation: This involves heating discharged LIBs to 100–150 ◦C for an hour prior to disassembly, which helps in regulated removal of the high-energy substances of spent LIBs, preventing unanticipated overheating [87,88].

3.2.3 Electrolyte extraction for direct recycling

The aforementioned procedure employs either supercritical or subcritical carbon dioxide to segregate the cathode and anode constituents of depleted LIBs, preparing them for subsequent utilization in remanufacturing. Notwithstanding its advantages, this method's effectiveness is limited by the state-of-health (SOH) of the spent LIB and other specific considerations [90,91].

3.3 Dismantling and Comminution

Once the Lithium-Ion Battery (LIB) is stabilized, it's subject to further processing which broadly falls into two categories: Dismantling and Comminution.

3.3.1 Dismantling

Manually disassembling expended batteries often involves simple tools, with limited safeguards in place to address potential hazards. Notably, disassembly of LIBs results in organic material leakage, predominantly dimethyl carbonate (DMC) and tert-amylbenzene. Specialized methodologies, like the Z-folded separators, are required to manage the allowable DMC quantities. Innovations such as the Battery Identity Global Passport bolster these efforts by enabling battery identification via radio frequency identification (RfID) tags and QR codes. Yet, full automation remains elusive due to the diversity of LIB designs and potential damage to fasteners over the battery's lifespan.

Dismantling raises several complexities:

a) Module and Cell Removal: The intricate battery structure, with numerous cells contributing to its high output, poses a significant dismantling challenge. Different manufacturers use a variety of configurations, creating a unique collection of connectors, screws, and adhesives for each battery. Careful dismantling is crucial, given the hazards associated with fluorine-rich waste materials.

b) Casing Removal: The casing, designed to protect battery elements, isn't optimized for end-of-life recycling. Opening it is laborious and poses risks such as short-circuits, increasing labor costs and posing potential risks to the workers.

c) Wire Removal: Disentangling the critical wiring network, differing per manufacturer, is a painstaking and time-consuming process that complicates manual disassembly. Wire condition variability hampers AI or machine learning applications.

d) Glue Removal: Glue, essential for battery pack rigidity, is often dissolved using organic solvents. However, due to solvent composition and the time involved, this hinders the feasibility of recycling through disassembly.

e) Binder Removal: Removing the binder, which attaches the active material to the current collector foil, presents a further disassembly hurdle. While binders like Polyvinylidene Fluoride (PVDF) have been traditionally used for their electrochemical stability and binding properties, their removal through pyrolysis or dissolving creates harmful waste. Although alternatives are being explored, the existing batteries still have PVDF, requiring appropriate disposal methods.

3.3.2 Comminution

Comminution, or mechanical disintegration of the battery packs into a metal-enriched black material, provides an alternative to dismantling. The comminution process, inclusive of shredding, hammer milling, and granulating, can result in materials with varying size and shape, influencing downstream separation strategies.

a) Dry Crushing: Crushing LIBs without water, or dry crushing, is popular in many industrial facilities. This process involves batch crushing of sorted used LIBs for consistency. While devoid of chemical reagents and boasting high separation efficiencies, it may be laborious, costly, and demand a dust prevention system. To ensure safety, innovative crushing methods have been developed in cryogenic or inert conditions, using gases like argon, nitrogen, and carbon dioxide to prevent spontaneous burning or hazardous gas generation.

b) Wet Crushing: Crushing LIB components in water, or wet crushing, neutralizes the reactivity of lithium, aids in dust prevention, and serves as a heat sink to prevent explosions. Despite its advantages, this approach generates hard-to-handle wastewater, adding operational expenses.

While dismantling results in purer output, the process can be challenging, time-consuming, and costly. Conversely, comminution offers a more straightforward and uniform handling process but results in less purified to focus on the User request.

3.4 Separation

Post-disassembly and comminution processing yield high-grade material feedstocks through physical separation. This procedure delivers concentrated feedstocks for further refining stages, such as metal dissolution and deposition. The separation outcomes include plastic, separator and pouch material, metals, steel casing, Ni and Al tabs, Al and Cu current collectors, and a composite of other constituents. The composite is primarily comprised of components from the anode and cathode, and is earmarked for subsequent refining. The cost-effectiveness of subsequent procedures is largely contingent upon the purity of separated feedstocks. Thus, a proficient physical separation stage is critical to curtail purification requirements and operational costs.

3.4.1 Sieving/particle size separation

All large-scale LIB recycling protocols employ sieving to segregate particles based on size. This technique isolates composite material constituents, such as electrode coatings, graphite, and metal oxides. Recovery efficiency for various elements reportedly improves by 10% post-particle separation.

3.4.2 Magnetic separation

The removal of steel casings and other ferrous materials is accomplished through magnetic separation. Diverse streams of active material are produced when mixed components are consolidated into a slurry and exposed to varying magnetic intensities. Using this technique, also known as "direct recycling," the active component is kept in its oxide form. It is successful in mixed cell feed recycling for cathode extraction despite certain difficulties with economic viability and trouble separating various nickel, manganese, and cobalt ratios.

3.4.3 Electrostatic separation

This technique uses variations in conductivity to distinguish metallic fractions and polymers. In contrast to magnetic attraction that occurs naturally, electrostatic separation charges particles to encourage separation. Following separation, the metallic fraction has a metal content of 98.98% whereas the nonmetallic fraction has a polymer content of 99.6%. Recirculating composite parts through the sorting procedure can improve purification even more.

3.4.4 Eddy current separation

Pre-separation based on differential physical properties improves the recycling efficiency of spent LIBs. Eddy current separation, utilized for recycling lithium iron phosphate batteries, Cu, and Al, is based on different conductivities. By generating eddy currents in nonferrous metals through a magnetic field, non-ferrous metals are isolated from the rest. After discharge and deconstruction, the LIBs are crushed to free each component for separation.

3.4.5 Gravity/density separation

This technique, which is effective for processing used LIBs, divides components depending on their densities. Low-density plastics and papers may be successfully separated from mixed cell waste using gravity/density separation fluidized bed processing. Metal is separated from plastic and biological materials using sophisticated density separation processes including jigging and hydrocyclones.

3.4.6 Froth flotation

Using froth flotation, it is effective to separate minute particles according to how hydrophilic their surfaces are. Bubbles pick up hydrophobic things and carry them to the surface where they may be collected. Due to the hydrophobic PVDF binder sticking to the electrode powders, this approach initially faced difficulties with poor selectivity amongst electrode particles. However, employing heat to disintegrate and remove PVDF makes it possible to successfully recover carbons via froth flotation from cathode materials.

3.5 Pyrometallurgy Route:

Through various thermal treatments, pyrometallurgy is a technique that makes use of high temperatures to recover valuable metals from used lithium-ion batteries (LIBs). The LIBs components can either be put straight into a smelting furnace or can undergo pretreatment processes to recover the active cathode material [63]. While the enhanced metallic fraction of LIBs is recovered through roasting, calcination, and smelting, some procedures utilized to recover cathode materials include incineration, calcination, and pyrolysis [64]. These post-treatment procedures for pyrometallurgical recycling of used LIBs are shown in Table 3.2. It is not frequently advised to smelt used LIBs since it can be difficult to recover some metals, notably Li and Al. Fig. 3.2 depicts a straightforward process flow diagram for the pyrometallurgical recycling of LIBs. Due to chemical reactions predominating in high-temperature activities, slag, CO2, and dangerous gases including dioxins and furans are produced [65]. In contrast, lowering the operation temperature alters the feed's structure and generates phase transitions, which leads to the pyrolysis-induced destruction of organic materials and graphite. Li is highly reactive in these conditions, thus air and moisture are removed from the system using vacuum.

Using carbon black, pyrolytic carbon, and hydrogen fluoride to pyrolyze $LiCoO_2$, [66] were able to produce CoO, Li2CO3, LiF, and Li_2O at a temperature of 600 °C. They discovered that following water leaching, there was a 92% recovery of Li. The utilization of microwave-assisted pyrolysis offers a variety of perks such as swift heating speeds, exceptional metal preference, consistent heating, effortless power regulation, and amplified degradation kinetics [67]. Furthermore, during the carbothermic reductive roasting process, agents such as carbon, charcoal, or coke are used which leads to heating of the active cathode material. A mixture of impure alloys and a carbon residue are produced as a result of the process, which is then refined further. Double redox reactions occur at lower temperatures when carbon is present, which enhances the reduction process [68].

Table 3.1 : A brief rundown of the pyrometallurgical technique used for recycling spent lithium ion batteries.

Process Type	Additive	Pretreatment	Thermal Processing	Recovery Rate (%)
Vacuum prolysis	-	Discharging, dismantling, separating	600 °C, 30 min	99 Co, 99 Li
Oxygen-free roasting	Carbon	-	1000 °C, 30 min	95.72 Co, 98.93 Li
Reduction roasting	Graphite	Discharging, crushing, Pneumatic separation	600 °C, 120 min	100 Li, 100 Co
Sulfation roasting	SO_2 (gas)	-	700 °C, 120 min	99.5 Li, 17.4 Co
Nitration roasting	HNO_3	Mechanical pretreatment	250 °C, 60 min	92 Co, 93 Li
Chlorination calcination	NH_4Cl	Discharging, manual dismantling, NaOh dissolution	350 °C, 20 min	99.18 Li, 99.3 Co
Ammonium sulfation roasting	$(NH_4)_2SO_4$	NaCl discharging, manual dismantling, muffle furnace heating	400 °C, 120 min	98 Li, 98 Co
Chlorination roasting	Cl_2 (gas)	NaCl discharging, dismantling, HNO_3 leaching	900 °C, 90 min	100 Li, 100 Co
Pyrolysis	N_2	Crushing, disassembling	500 °C, 90 min	87.5 Li, 99.18 Co

According to [69], lithium cobalt oxide (LCO) is stable at temperatures below 850°C. They claimed that at temperatures above 300°C, reducing substances like carbon and oxygen can decrease metal oxide through the following reactions:

$$4\ LiCoO_2(s) + 3\ C(s) \rightarrow 2\ Li_2O(s) + 4\ Co(s) + 3\ CO_2\ (g) \tag{3.1}$$

$$4\ LiCoO_2(s) + C(s) \rightarrow 2\ Li_2O(s) + 4\ CoO(s) + CO_2\ (g) \tag{3.2}$$

$$2\ LiCoO_2(s) + 3\ C(s) \rightarrow Li_2O(s) + 2\ Co(s) + 3\ CO\ (g) \tag{3.3}$$

$$2\ LiCoO_2(s) + C(s) \rightarrow Li_2O + 2\ CoO(s) + CO\ (g) \tag{3.4}$$

$$2\ LiCoO_2(s) + 3\ CO\ (g) \rightarrow Li_2\ O(s) + 2\ Co(s) + 3\ CO_2\ (g) \tag{3.5}$$

When a lithium-ion battery is recycled using pyrometallurgical methods, lithium creates a stable oxide, Li_2O, and maintains its oxidation state, according to [69]. Cobalt can, however, be changed into Co_2+ or Co metal. The authors also proposed that the following reaction is the most advantageous from a thermodynamic perspective:

$$6LiCoO_2\ (s) + 5C(s) \rightarrow 6Co(s) + 3Li_2CO_3\ (s) + CO\ (g) + CO_2 \tag{3.6}$$

A multi-vacuum-pyrolysis procedure was suggested by [67] as an eco-friendly method of recycling lithium-ion batteries without the use of potentially harmful chemicals. They also talked about how Li_2CO_3 and CoO can be used to regenerate $LiCoO_2$ in a solid state reaction. Lithium and cobalt from the LCO electrode feed were successfully separated using carbon as the reducing agent. The following equations can be used to understand the procedure:

$$4\ LiCoO_2 + C = Li_2O + Li_2CO_3 + 4\ CoO \tag{3.7}$$

$$Li_2O + 2CoO + C = 2\ Co + Li_2CO_3\ (g) \tag{3.8}$$

The reactions shown previously by [69] occur spontaneously at temperatures above 146°C. This process was found to be efficient, with an approximate recovery rate of 93% for lithium and 99% for cobalt through vacuum pyrolysis followed by carbothermic reduction and water leaching. This process not only delivers a high yield in metals recovery but also an environmentally friendly solution for recycling spent lithium-ion batteries.

For the treatment of used lithium-ion batteries, [70] created a process that combines wet magnetic separation with oxygen-free roasting. Li et al. found that significant reactions between lithium cobalt oxide (LCO) and graphite take place at 1000 °C for 30 minutes in an oxygen-free environment. This method offers a way to recover precious metals while reducing the environmental impact of disposing of discarded LIBs.

$$4\ LiCoO_2 + 2\ C \rightarrow 4\ Co + 2\ Li_2CO_3 + O_2\ (g) \tag{3.9}$$

$$2\ LiCoO_2 + 2\ C \rightarrow 2\ Co + Li_2CO_3 + CO\ (g) \tag{3.10}$$

$$4\ LiCoO_2 + 3\ C \rightarrow 4\ Co + 2\ Li_2CO_3 + CO_2(g) \tag{3.11}$$

The researchers in [70] noted that the concluding residue of the process, which encompasses oxygen-free roasting coupled with wet magnetic separation, is composed of a blend of cobalt, graphite, and LCO. Post the wet magnetic intervention, they ascertained recovery rates for Li, Co, and graphite at 95.72%, 98.93%, and 91.05% respectively. This methodology proves cost-effective due to the minimal chemical involvement, paving a theoretical route for recycling lithium-ion batteries on an industrial scale. Nevertheless, despite its efficacy in the retrieval of high-value metals, a principal drawback of this approach is the generation of hazardous gases, akin to the repercussions of pyrometallurgical pathways. The succeeding segment evaluates an alternative technique that promises a safer and more environmentally sustainable recycling process.

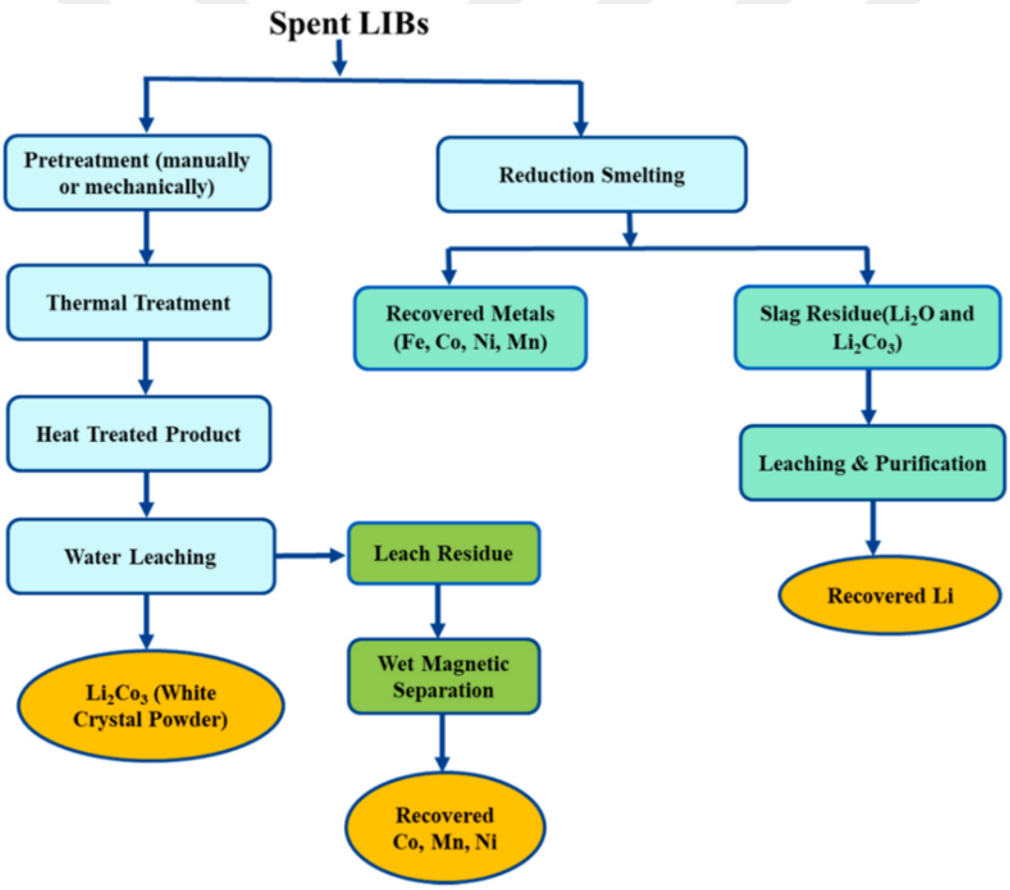

Figure 3.2 : An illustration of the pyrometallurgical route used to extract Li and Co from LIBs, as described in sources [63].

3.6 Hydrometallurgy Route

The main steps of the pyrometallurgical approach for recycling used lithium-ion batteries (LIBs) were covered in the section prior. As previously mentioned, a combination of hydrometallurgical methods is required to successfully recover valuable metals from used electrodes. Among these approaches is the use of liquid extraction to recover metals, followed by the use of purification and recovery techniques such selective precipitation, ion exchange, solvent extraction, and contemporary membrane technologies to separate valuable metals from the leach fluid [71,72]. The hydrometallurgical method's crucial processes are dissolving, separating impurities, extracting lithium, and recovering other metals. The hydrometallurgical approach to treating used LIBs is shown in the flowchart in Figure 3.3. Spent LIBs contain materials including Li, Mn, Ni, Co, and Al. In alkaline circumstances, some of these compounds can be removed more effectively. Using a combination of hydrometallurgical processes to recycle used LIBs offers a workable and sustainable alternative.

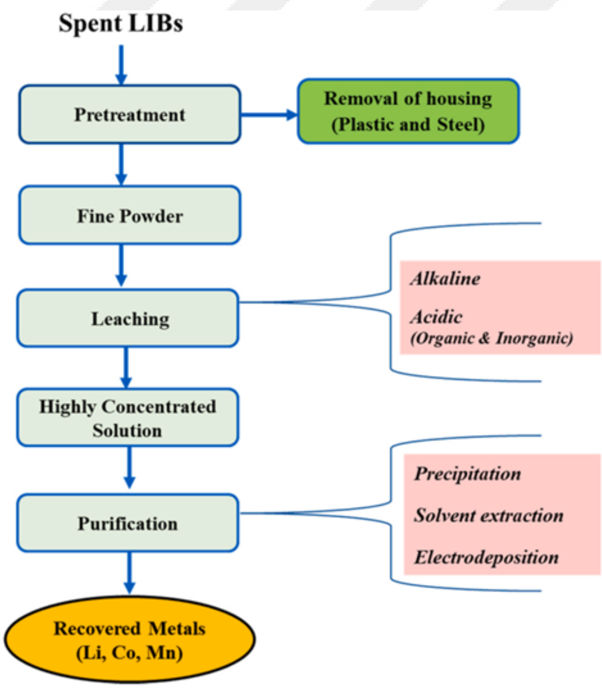

Figure 3.3 : Illustration of hydrometallurgy process for the spent LIBs [73].

Recovering metallic values from spent lithium-ion batteries (LIBs) can involve multiple methods, including a two-step process of alkaline leaching followed by acidic leaching. By offering an ideal starting product for the subsequent acid dissolving procedure, the method makes it possible to remove aluminum from the electrode material. NaOH aqueous solution is commonly used for alkaline leaching. This method makes it feasible to extract the most aluminum and other metals from the battery electrode material. Despite not being dissolved, the other metals are still retained in the solid waste left over after filtering the leach liquid. Thus, in order to handle used LIBs in a zero-waste manner, scientists are focusing on inorganic or organic acid dissolving methods. Not only does this technique extract the valuable metals, but it also decreases the ecological footprint and reduces the cost of waste management.

3.6.1 Leaching of LIBs with inorganic acids

There has been extensive research on the use of acidic leaching with inorganic acids such H_2SO_4, HCl, and HNO_3 for the extraction of precious metals from used lithium-ion batteries (LIBs). Leaching reactions can be accelerated and metal extraction rates from utilized LIBs can be increased by using strong acids with high dissociation constants in conjunction with reducing agents or halides. Sulfuric acid is the inorganic acid that is most frequently utilized in the leaching of precious metals from waste sources (H_2SO_4). Several research teams have revealed that key elements like Li and Co may be leached from used LIBs with high efficiency using sulfuric acid. According to [74], they found that by utilizing H_2SO_4 leaching of spent LIBs, they could recover up to 98% of the Li and Co that were dissolved in the solution, but the process might take up to 6 hours to complete. Leaching time was found to be decreased in the presence of H_2O_2, while leaching efficiency was found to be decreased, according to [75] .99% lithium and cobalt recoveries were reported by [76] using a 2 M sulfuric acid solution at 80°C for 60 minutes with a solid/liquid ratio of 50 g/L. Additionally, H2O2 is added to speed up the process and increase leaching efficiency.

$$2\ LiCoO_2 + 3\ H_2SO_4 + H_2O_2 \rightarrow Li_2SO_4 + 2\ CoSO_4 + 4\ H_2O + O_2 \tag{3.12}$$

According to Ferreira and colleagues [77], the solid residue obtained after dissolving LCO batteries with sulfuric acid contained cobalt oxide (Co3O4) (H2SO4). To convert Co3O4 into soluble $CoSO_4$, an excess of H_2SO_4 is necessary to facilitate the sequential reaction as follows:

$$4LiCoO_2 + 3\ H_2SO_4 \rightarrow Co_3O_4 + 2\ Li_2SO_4 + CoSO_4 + 3\ H_2O + 1/2\ O_2 \tag{3.13}$$

$$Co_3O_4 + 3\ H_2SO_4 \rightarrow 3\ CoSO_4 + 3\ H_2O + 1/2\ O_2 \tag{3.14}$$

Overall balanced reaction:

$$3\ LiCoO_2 + 6\ H_2SO_4 \rightarrow 2\ Li_2SO_4 + 4\ CoSO_4 + 6\ H_2O + O_2 \tag{3.15}$$

The extraction rate of lithium was found to be 100% and that of cobalt to be 97% in this study using sulfuric acid (H_2SO_4). [78] also investigated the effects of sodium metabisulfite ($Na_2S_2O_3$) and hydrogen ion (H^+) concentration on the dissolving rate of cobalt, copper, and lithium and observed that as sodium metabisulfite concentration increases, the leaching rate for these metals decreases. The ideal leaching conditions were reported to be 3 M H_2SO_4, 15:1 liquid/solid, 0.25 M $Na_2S_2O_3$, 90°C, and 3 hours. Lithium and cobalt were recovered at 99.71% and 99.95%, respectively, under these circumstances. The following are the leaching reactions:

$$8LiCoO_2 + Na_2S_2O_3 + 11H_2SO_4 \rightarrow 4Li_2SO_4 + 8CoSO_4 + Na_2SO_4 + 11H_2O \quad (3.16)$$

[79] reported that optimal conditions for extracting lithium and cobalt from electrode waste through leaching with hydrochloric acid (HCl) solution are: 2 M HCl, 60-80°C and 90 minutes. They found that this method is more effective than using sulfuric acid (H_2SO_4). They stated that the following is how lithium and hydrochloric acid react chemically:

$$2LiCoO_2 + 8\,HCl \rightarrow 2\,LiCl + 2\,CoCl_2 + 4\,H_2O + Cl_2 \quad (3.17)$$

Using HCl as the leaching solution, [73] demonstrated a good recovery rate of lithium, manganese, cobalt, and nickel from used LIBs. They discovered that recovery of 96 weight percent lithium, 98 weight percent manganese, 96 weight percent cobalt, and 97 weight percent nickel with at least 96% purity was possible under the ideal conditions of 4 M HCl solution, 80 ^{o}C, 1 hour of leaching time, and a solid-to-liquid ratio of 0.02 g/l. Furthermore, [80] reported 100% lithium leaching efficiency using HNO_3, while other researchers have found HNO_3 to be effective as well with the addition of H_2O_2, which accelerates chemical reactions and reduces leaching time. The experimental setup and outcomes of using various inorganic acids to dissolve lithium and cobalt from used LIBs are summarized in Table 3.4 of the study, with the authors arriving at the conclusion that sulfuric acid (H_2SO_4) is effective at dissolving a variety of metals, including lithium and cobalt. However, other acids, such as nitric acid (HNO_3) and hydrochloric acid (HCl), can also be used to speed up the leaching process because of HCl's strong reducing power, which increases leaching effectiveness.

3.6.2 Leaching of LIBs with organic acids

Due to their minimal fume production and environmental friendliness, organic acids have been shown to be a superior alternative to inorganic acids for the leaching of metals from LIBs. Citric acid and L-aspartic acid are two examples of organic acids that have been discovered to be effective at high pulp densities and to have relatively high leaching efficiencies [81]. The authors have concluded that organic acids are capable of achieving decent leaching results, with 100% leaching of metals. Li and colleagues have also performed ascorbic acid leaching experiments, [82] revealing leaching efficiencies of 94.8% and 98.5% for cobalt and lithium, respectively, using concentration ranges of 0.3-1.5M of ascorbic acid, under 50 minutes of leaching at temperatures between 30-90°C, with stirring at 300 rotations per minute. In addition, water leaching after roasting of LIB feed has also been found to be effective. Crystallization of Li_2CO_3 through evaporation method can also be used for lithium recovery [83].

[84] proposed utilizing ultrasonics to enhance $LiCoO_2$ leaching. They recommended 1.5 M DL-malic acid, 3 vol% H_2O_2, 4 g/L solid to liquid ratio and 95W ultrasonic power at 80°C for 25 minutes. Addition of H_2O_2 increased cobalt dissolving and thus obtaining high extraction rates of 99% Li and 93% Co.

$$2LiCoO_2 + 6C_4H_6O_5 + H_2O_2 \rightarrow 2LiC_4H_5O_5 + 2Co(C_4H_5O_5)_2 + 4H_2O + O_2 \quad (3.18)$$

$$6C_4H_6O_5 + 2LiCoO_2 + H_2O_2 \rightarrow 2LiC_4H_5O_5 + 2Co(C_4H_5O_5)_2 + 4H_2O + O_2 \quad (3.19)$$

$$6C_4H_5O^{-5} + 2LiCoO_2 + 2Li^+ + 2\ Co_2^+ + H_2O_2 \rightarrow 2Li_2C_4H_5O_5 + 4CoC_4H_5O_5 + H_2O + 2.5O_2 \quad (3.20)$$

To achieve 98% $LiCoO_2$ leaching efficiency, [85] suggested an environmentally benign approach that combines vacuum pyrolysis, oxalic acid ($H_2C_2O_4$) leaching, and precipitation. Additionally, the process employs a hydrometallurgical method for the separation of lithium and cobalt. The chemical reactions for this process were also specified.

$$2\ LiCoO_2 + 7\ H2C_2O_4 \rightarrow 2\ LiHC_2O_4 + 2\ Co(HC_2O_4)_2 + 4\ H_2O + 2\ CO_2 \quad (3.21)$$

$$2\ LiCoO_2 + 4\ H_2C_2O_4 \rightarrow Li_2C_2O_4 + 2\ CoC_2O_4 + 4\ H_2O + 2\ CO_2 \quad (3.22)$$

[84] suggested an ultrasonic-boosted dissolving method for LiCoO2 materials by utilizing DL-malic acid, hydrogen peroxide, and ultrasonic energy, which achieved exceptional dissolving rates of 99 weight % Li and 93 weight % Co. [85] also presented an environmentally friendly process utilizing vacuum pyrolysis, oxalate leaching, and precipitation with 98% leaching efficiency for $LiCoO_2$. However, the use of organic acids may require a high volume of water and have higher operational costs compared to inorganic acids, as discussed in Table 3.3.

Table 3.2 : Collection of studies on the use of organic acids to dissolve LIBs and extract Li and Co**.**

Chemical Leaching Agent	Process Parameters	Li Efficiency (%)	Co Efficiency (%)
Ascorbic acid	Ascorbic 1.25 M, Time=20min, Temperature= 70°C	98	95
Ascorbic acid + Iminodiacetic acid	Iminodiacetic acid= M, Ascorbic acid 0.02 M, Time= 360 min, Temperature= 80 °C	99	91
Ascorbic acid + Citric acid	Citric acid - 0.1 M, Ascorbic acid = 0.02 M, Time= 360 min, Temperature= 80 °C	100	80
Citric acid + H_2O_2	Citric acid - 2M, H2O2 - 1.25 vol%, Time= 300 min, Temperature= 60 C	99.80	96.46
Oxalic acid + H_2O_2	Oxalic acid= 1 M, H2O2 = 15 vol%, Time= 120 min, Temperature= 80 °C	98	68
Asparatic acid + H_2O_2	Asparatic acid= 1.5 M, H2O2 - 4 vol%, Time= 120 min, Temperature= 90 °C	60	60
Malic acid + H_2O_2	Malic acid = 1.5 M, H2O2 - 24 vol%, Time= 40 min, Temperature= 90 °C	100	90
Malic acid + ascorbic acid	Malic acid = 1 M, ascorbic acid= 0.02 M, Time= 360 min, Temperature= 80 °C	100	97
Tartaric acid + Ascorbic acid	Tartaric acid 0.4 M, Ascorbic acid 0.02 M, Time 300 min, Temperature= 80°C	100	97
Methane sulfonic acid + H2O2	Methane sulfonic acid = M, H2O2 - 0.9 vol%, S/L ratio= 20 g/1, Time 60 min, Temperature=70 C	100	100
Phosphoric acid and citric acid	phosphoric acid= 0.2 M, citric acid= 0.4 M, Time= 30 min, Temperature= 90	100	91.63
DL malic acid + H_2O_2	DL Malic acid = 1.5 M, H2O2 = 3 vol%, S/L ratio= &, Time= 25 min, Temperature= 80 °C	98.13	98.86

Table 3.3 : Inorganic acidic leaching of LIBs for the recovery of valuable metals.

Chemical Leaching Agent	Process Parameters	Li Efficiency (%)	Co Efficiency (%)
H_2SO_4	H_2SO_4=3M, S/L ratio= 0.2g/l, Time= 360 min, Temperature= 70°C	98	98
H_2SO_4+H_2O_2	H_2SO_4 = 2M, S/L ratio = 100 8/1, H_2O_2 = 5 vol%, Time= 30 min, Temperature= 75 °C	94	93
H_2SO_4+H_2O_2	H_2SO_4 = 2M, H_2O_2 = 6 vol%, Time= 60 min, Temperature=60	97	98
H_2SO_4+H_2O_2	H_2SO_4 1 M, H_2O_2 - 1 vol%, Time= 60 min, Temperature= 40°C	99.7	99.7
H_2SO_4+H_2O_2	H_2SO_4 = 2M, H_2O_2 - 10 vol%, Time= 90 min, Temperature=70	99.76	98.46
H_2SO_4+H_2O_2	Liquid/solid ratio=10:1, Time 120 min, Temperature= 85 °	96	95
H_2SO_4 + H_2O_2	H_2SO_4 = 2.5 M, H_2O_2 - 3.3 vol%, Time= 150 min, Temperature=90	99	99
H_2SO_4+NaCI	H_2SO_4 = 1 M, NaCl = 0.2 M, Time= 120 min, Temperature= 30 C	90	90
H_2SO_4 + Glucose	H_2SO_4 = 2M, Glucose addition=5ml, Time 120 min, Temperature= 80 °C	92	88
H_3PO_4+H_2O_2	Acid Concentration - 0.7 M, H_2O_2 = 4 vol%, L/S ratio 20 ml/g, Time 60 min, Temperature= 40°C	99	99
HCI	HCI 4M, Time 120 min, Temperature= 80 °C	97	99
HCI	HCI 3 M, S/L ratio= 20 g/l, Time 90 min, Temperature= 80°C	99.4	-
HCI	HCI SM, S/L ratio 10g/, Time= 70 min, Temperature=95	98	99
HNO	HNO_3 - 2M, Time= 120 min, Temperature=80 C	100	-
HNO+H_2O_2	HNO_3 = 1 M, H_2O_2 - 1.7 vol%, S/L ratio= 10g/, Time= 30 min, Temperature=75 °C	100	100
HNO+H_2O_2	HNO_3 = 1 M, H_2O_2 = 1 vol%, Initial S/L ratio=20g/1, Time= 60 min, Temperature= 80 °C	100	100
HNO_3	HNO_3 = 3 M, Time= 30 min, Temperature= 90°C	-	98.01
HNO_3	HNO_3 = 10M, S/L ratio= 100g/1, Time= 30 min, Roasting Temperature= 275 °C	80	-

3.7 Bio Leaching Route

Microorganisms and their byproducts have been investigated as an environmentally benign alternative to pyrometallurgy and hydrometallurgy for the extraction of metals from used lithium-ion batteries (LIBs). Environmental friendliness, low gas generation, cheap operating costs, and a reduced need for energy are all benefits of bioleaching. A slower kinetics, however, is a significant drawback. Various scientists have looked into the bioleaching of LCO-type LIBs, and they've discovered that some bacteria, such Acidithiobacillus ferrooxidans, exhibit distinct feed and media reactions. Some microbes eat sulfur and ferrous ions to make byproducts like sulfuric acid and ferric ions, which can be utilized to dissolve the material. While Co recovery is higher when the proportion of S and FeS_2 is changed, Li leaching is more pronounced when sulfur serves as the primary energy source in the medium. Pulp density has an impact on bioleaching efficiency, with 2% pulp density achieving the highest recovery [86].

A recovery rate of 60% for lithium and 94% for cobalt was reported employing Acidithiobacillus ferrooxidans bacteria with a pulp density of 100 g/L over a 72-hour period in a study [33] . A variety of used LCO batteries were used for the research. In the study, the beneficial chemical reactions are described.

$$4\ LiCoO_2 + 12\ H^+ \rightarrow 4\ Li^+ + 4\ Co^{2+} + 6\ H_2O + O_2 \tag{3.23}$$

$$Fe^{2+} + LiCoO_2 + 4\ H^+ \rightarrow Fe^{3+} + Co^{2+} + Li^+ + 2\ H_2O \tag{3.24}$$

$$2\ FeSO_4 + 2\ LiCoO_2 + 4\ H_2SO_4 \rightarrow Fe_2(SO_4)_3 + 2\ CoSO_4 + Li_2SO_4 + 4\ H_2O \tag{3.25}$$

4. THERMODYNAMIC INVESTIGATION AND ANALYSIS

4.1 Roasting Thermodynamics

The compound $LiNi_{0.5}Co_{0.2}Mn_{0.3}O_2$ has a structure similar to that of α-$NaFeO_2$, which is a complex mixture of multi metal transitions. The method of reducing this compound through roasting is known to be intricate. Essentially, the disintegration reactions and resulting reduction products at various temperatures must be thoroughly understood before appropriate roasting conditions can be established. In a real-world manufacturing environment, In a pyrolysis heater, the cathode and anode electrode sheets are put for simultaneous decomposition. Aside from that, contamination from the electrode sheets must be avoided by maintaining the roasting temperature below the aluminum melting point (660 ^oC). Finding the viability, course, and make-up of reactions at various temperatures can be aided by a thermodynamic analysis of the roasting process. Table 4.1 from the works of [87–90] lists the possible reactions that could take place during the mixed roasting of $LiNi_{0.5}Co_{0.2}Mn_{0.3}O_2$ and charcoal powder. Diagrams in Fig. 4.1 show the G T of these processes. [91] provided information on the nickel cobalt lithium manganate's thermodynamic properties, and Fact Sage 8.0, HSC 6.0, and Physical Chemistry provided additional thermodynamic information. Figure 4.1 shows that when reaction mentioned reaches a temperature of 730 K, the "G" value is zero, and as the temperature rises, the "G" value turns negative and the reaction proceeds spontaneously. Similar to reaction 1-2, reaction 1-3 occurs spontaneously at temperatures between 100 and 1000 K where the G value is always negative while reaction 1-2 has a G value of 0. Reaction 1-3 has a G value of 0, and as temperature rises, the G value becomes negative. In conclusion, the analysis and computation of the thermodynamic properties show that $LiNi_{0.5}Co_{0.2}Mn_{0.3}O_2$ can be spontaneously transformed to metal oxides of lithium, nickel, cobalt, and manganese as well as carbon and carbon monoxide at temperatures between 730 and 1000 K.

Additional reactions may occur between carbon and carbon monoxide with the metal oxides generated in the previous steps, as outlined in reactions 1-4 to 1-9. The thermodynamic analysis, as described in works by [87–90] shows that the $\Delta G\theta$ values of reactions 1-4, 1-5, 1-7, and 1-8 are negative in the temperature range of 100-1000K, indicating that these reactions can occur spontaneously. However, the ΔGθ value of reaction 1-6 is positive in the same temperature range, indicating that the reaction is not thermodynamically favorable and cannot proceed spontaneously. Additionally, for reaction 1-9, when the temperature is below 708K, the ΔGθ value is negative, indicating spontaneous reaction. But at temperatures higher than 708K, the ΔGθ is positive, the reaction is not likely to happen spontaneously.

Table 4.1 : Possible reactions of $LiNi_{0.5}Co_{0.2}Mn_{0.3}O_2$ + C.

Reaction	ΔG(kJ.mol^{-1})	No
$2Li(Ni_{0.5}Co_{0.2}Mn_{0.3})O_2 + 05C \rightarrow Li_2O + NiO + 0.4CoO + 0.6MnO + 0.5CO_2$	ΔG = 38 - 0.079 T	1-1
$2Li(Ni_{0.5}Co_{0.2}Mn_{0.3})O + C \rightarrow Li_2O + NiO + 0.4CoO + 0.6MnO + CO$	ΔG = 124.2 - 0.17 T	1-2
$2Li(Ni_{0.5}Co_{0.2}Mn_{0.3})O_2 + CO \rightarrow Li_2O + NiO + 0.4CoO + 0.6MnO + CO_2$	ΔG = -48.227 + 0.0009 T	1-3
$C + 2NiO + Li_2O \rightarrow 2Ni + Li_2CO_3$	ΔG = -120.8 + 0.03 T	1-4
$C + 2CoO + Li_2O \rightarrow 2Co + Li_2CO_3$	ΔG = -140.14 - 1.3x10^{-3} T	1-5
$C + 2MnO + Li_2O \rightarrow 2Mn + Li_2CO_3$	ΔG = 151.9 + 8.6x10^{-3} T	1-6
$CO + NiO + Li_2O \rightarrow Ni + Li_2CO_3$	ΔG = -258.855 + 0.153 T	1-7
$CO + CoO + Li_2O \rightarrow Co + Li_2CO_3$	ΔG = -268.525 + 0.168 T	1-8
$CO + MnO + Li_2O \rightarrow Mn + Li_2CO_3$	ΔG = -122.505 + 0.173 T	1-9
$2Li(Ni_{0.5}Co_{0.2}Mn_{0.3})O_2 + 1.2C \rightarrow Li_2CO_3 + Ni + 0.4Co + 0.6MnO + 0.2CO_2$	ΔG = -117.76 - 0.047 T	1-10
$2Li(Ni_{0.5}Co_{0.2}Mn_{0.3})O_2 + 1.2C \rightarrow Li_2CO_3 + Ni + 0.4Co + 0.6MnO + 0.4CO$	ΔG = -83.27 - 0.082 T	1-11
$2Li(Ni_{0.5}Co_{0.2}Mn_{0.3})O_2 + CO \rightarrow Li_2CO_3 + Ni + 0.4Co + 0.6MnO + O_2$	ΔG = 71.467 - 0.018 T	1-12

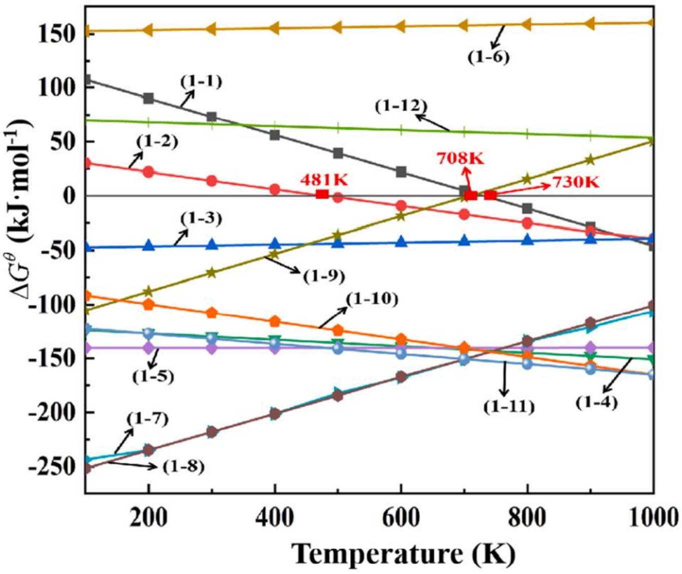

Figure 4.1 : ΔGθ − T Diagram for the reduced roasting of used ternary cathode materials.

The simultaneous pyrolysis of $LiNi_{0.5}Co_{0.2}Mn_{0.3}O_2$ and carbon at temperatures between 773 to 923 K has the ability to produce metal oxides, according to the thermodynamic analysis reported in research by [87–90]. It's crucial to remember that lithium oxide cannot be reduced; rather, lithium carbonate will be the result. Nickel oxide and cobalt oxide can be reduced further to their respective metallic states, nickel and cobalt, through the application of carbon and carbon monoxide. Contrarily, under these conditions, manganese oxide resists conversion to manganese, persisting in its original state. The oxygen atoms within the $LiNi_{0.5}Co_{0.2}Mn_{0.3}O_2$ lattice could react with carbon, generating either CO_2 or CO. If all reactions transpire completely and optimally, the final products of roasting $LiNi_{0.5}Co_{0.2}Mn_{0.3}O_2$ and carbon simultaneously would be lithium carbonate, nickel, cobalt, manganese oxide, and either carbon dioxide or carbon monoxide. The precise series of reactions are elaborated in equations 1-10 to 1-12. The Gibbs free energy values for reactions 1-10 and 1-11 within the temperature range of 100-1000K are negative, implying the potential for their spontaneous initiation. The G value, on the other hand, is positive for reaction 1–12 within the same temperature range, suggesting that the reaction will not occur on its own.

4.2 Leaching Thermodynamics

The link between reaction potential and pH value in an aqueous solution system can be seen using Eh-pH diagrams. Plotting the electrode potential on the vertical axis and the pH value on the horizontal axis under particular temperature, component activity, and pressure circumstances results in the diagrams [92]. These charts can be employed to illustrate the conditions for constituent equilibrium as well as the regions where the constituents are stable in an aqueous solution. They also offer an important thermodynamic foundation for the hydrometallurgical procedure in watery systems. In this instance, sulfuric acid was used to dissolve the roasting-related products. To find the ideal conditions for dissolving lithium, nickel, cobalt, and manganese metals in water at 85 °C, the software HSC 6.0 was used to create Eh-pH diagrams for each system (depicted in Fig. 4.2).

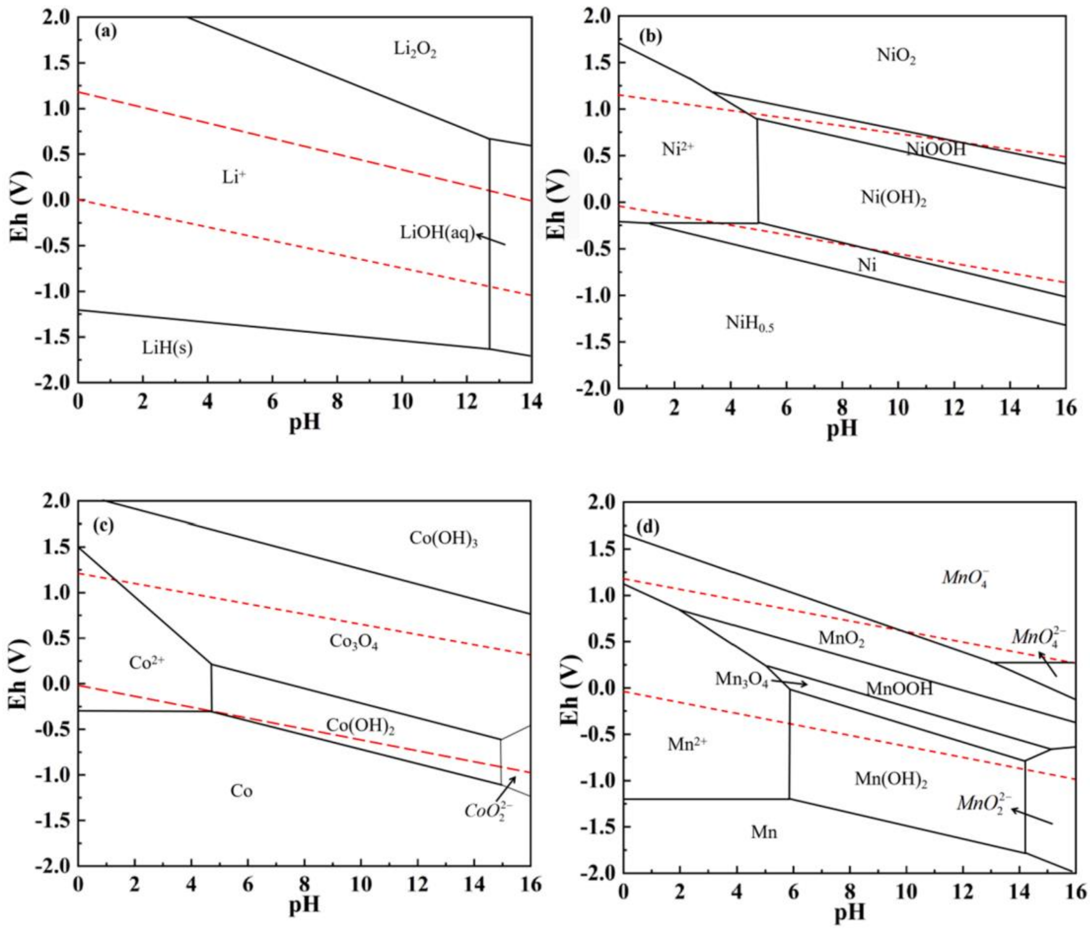

Figure 4.2 : Eh-pH diagrams of Metal-H_2O system at 85 ◦C.

Figure 4.2(a) shows that lithium does not exist in a stable form within the stable area for water, but rather is present as lithium ions in solution. Even while extremely alkaline conditions can be used to make lithium hydroxide, the size of this region suggests that alkaline systems are not a good option for lithium extraction. Figures 4.2b–d show that at 85 °C and a pH of less than 5, the stable areas of Ni, Co, and Mn in an aqueous solution system exist as Me^{2+}. Therefore, when the pH is less than 5 and the solution potential is between 0.25 V and 0.5 V, lithium, nickel, cobalt, and manganese from the roasting product can dissolve as metal ions in acidic circumstances, according to the analysis of the Eh-pH diagram for each of these elements. The following are the primary reactions that occur throughout the dissolving process:

$$Li_2CO_3 + H2SO4 \rightarrow Li_2SO_4 + H_2O + CO_2\uparrow \quad (4.1)$$

$$NiO + H2SO_4 \rightarrow NiSO_4 + H_2O \quad (4.2)$$

$$Ni + H_2SO_4 \rightarrow NiSO_4 + H2\uparrow \quad (4.3)$$

$$CoO + H_2SO_4 \rightarrow CoSO_4 + H2O \quad (4.4)$$

$$Co + H_2SO_4 \rightarrow CoSO_4 + H2\uparrow \quad (4.5)$$

$$MnO + H_2SO_4 \rightarrow MnSO_4 + H_2O \quad (4.6)$$

5. EXPERIMENTAL STUDY

This work aims to develop a selective process for the recovery of valuable metals, such as Li, Co, Ni, Cu, and Mn, from spent lithium-ion batteries (LIBs) through a combination of pyrometallurgy and hydrometallurgical leaching techniques. Through a literature review, two methods were selected: (1) a hydrometallurgical approach using HCl acid leaching on LIBs with a current of 3200mA, and (2) a pyrometallurgical method involving smelting and roasting of the material in induction and ash furnaces. The hydrometallurgical path involved separating electrode materials from the LIBs, leaching them in a hydrochloric acid solution for 2 hours at an average temperature of 85.5 ºC, and then analyzing the samples with atomic absorption spectrometry at different intervals (30 min., 60 min., and 120 min.). Results showed that the samples contained Mn, Cu, Ni, and Co. Meanwhile, in the pyrometallurgical path, samples of electrodes were roasted at incremental temperatures from 700 ºC to 1500 ºC in different furnaces for periods from 1 hour up to 3 hours. It was found that increasing the temperature rapidly to a certain degree between 1250 – 1350 ºC resulted in a direct metallic formation of the valuable elements, and the use of flux materials such as silica and borax prevented adhesive behavior between the sample and the ceramic crucible. This is an ongoing project, further experiments are planned to optimize the process for efficient recovery of valuable metals from spent LIBs.

5.1 Pre Experimental Analysis

Two portions of the spent LIBs were selected for analysis through the process of mechanical separation of the batteries. One portion was sent for X-ray fluorescence analysis of the aluminum casing, and the other portion was analyzed for structural analysis of the LIB insulators using Fourier-transform infrared spectroscopy (FT-IR).

5.1.1 XRF analysis of aluminum casings:

An X-ray fluorescence (XRF) analysis was conducted and it was determined that the type of aluminum casing used in the lithium-ion batteries (LIBs) is AA 3003. This series of aluminum sheet has excellent corrosion resistance and a good production technology. It is approximately 20% stronger than the 1100 series, yet maintains good workability. It reacts well to mechanical and organic finishing, but it may exhibit a minor discoloration when anodized. With the exception of the torch process, AA 3003 aluminum is easily brazed and welded. Because of its propensity to "gummy," it can be challenging to process. Heat treatment is not an option. Appliance parts, truck and trailer covering, heat exchangers, lawn furniture parts, and equipment for the food and chemical industries are some examples of the applications where it is frequently employed. The precise percentages of the casings' constituent elements are displayed in the table 5.1.

Table 5.1 : Elemental percentage of Aluminum casings of the batteries with XRF analysis.

AA 3003		
Element	%	±2σ
Al	97.023	0.162
Mn	1.264	0.038
Fe	1.133	0.029
Si	0.306	0.030
Cu	0.083	0.004
Zn	0.011	0.002
Zr	0.001	0.000

5.1.2 Structural analysis through FT-IR:

A Fourier-transform infrared spectroscopy (FT-IR) analysis was performed on the plastic insulators obtained from the spent lithium-ion batteries (LIBs) through mechanical separation to gain a deeper understanding of the material composition. The results of the test indicated that the examined insulators were identified as polypropylene (PP).

The graph above shows that the polyethylene and polypropylene bands present in the sample designated as P1 have been identified. The bands at 2949.45 cm-1, 2869.04 cm-1 and 2838.72 cm-1 correspond to the C-H stretching of the polypropylene. The band at 2918.37 cm-1 corresponds to the C-H stretching of both polypropylene and polyethylene. The band at 1455.52 cm-1 corresponds to the CH_2 band of polypropylene. The band at 1375.86 cm-1 corresponds to the CH_3 band of both polyethylene and polypropylene. The band at 1167.4 cm-1 indicates the CH stretching band, CH_3 vibrations, and C-C stretching. The band at 997.94 cm-1 corresponds to the CH_3 vibrations, CH_3 band, and CH band of polypropylene. The band at 971.14 cm-1 corresponds to the CH_3 vibrations and C-C stretching of polypropylene. The band at 840.6 cm-1 corresponds to the CH_2 vibrations and C-CH_3 stretching of polypropylene. The band at 808.59 cm-1 corresponds to the CH_2 vibrations, C-C stretching and C-CH stretching of polypropylene.

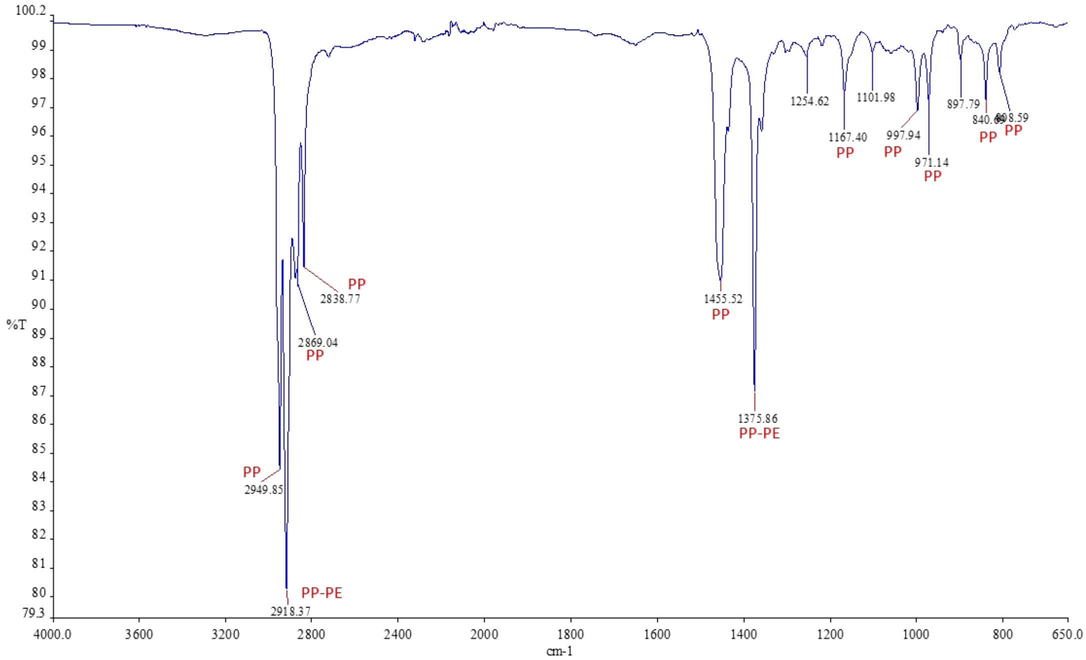

Figure 5.1 : FT-IR results of polymer layers attached; PE: Polietilen PP: Polipropilen.

5.2 Experimental Procedures

In this study, 20 Samsung lithium-ion batteries (LIBs) with a total weight of 692.9 grams were dismantled and separated from their aluminum casings. The weight percentage of each component was calculated and recorded. A quarter of the electrode material, weighing 112.3 grams, was extracted from the LIBs and placed in a beaker for leaching in a solution of hydrochloric acid (50% wt) and distilled water (50% wt) for 2 hours at an average temperature of 85.5 ^{o}C. Samples of 50 milliliters were taken at intervals of 30 minutes, 1 hour, and 2 hours for chemical analysis. The first two samples were taken from the initial solution using a dropper and transferred to small beakers for examination. The last sample was taken after the heating process was completed and was filtered, the solid cake containing the electrodes was dried in an oven for 12 hours before it was sent for separate chemical analysis. The samples taken from the leached solution were filtered to remove large particles and sent for chemical analysis. The dried leached cake was ground in a mill for 5 minutes to obtain a finer powder for X-ray diffraction (XRD) analysis, and the pure copper sheets were separated and the remaining sample was sent for analysis.

Figure 5.2 : 112.3 grams of electrode mixed in 500 mL hydrochloric acid and 500 mL of distilled water.

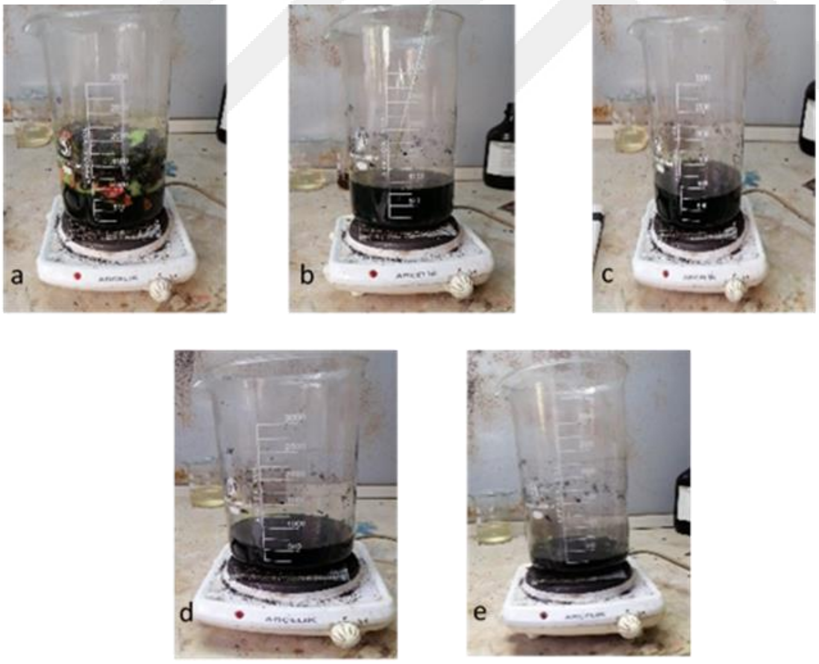

Figure 5.3 : Solutions at minute a) 0, b) 15, c) 30, d) 60 and e) 120 with a 500 mL containing 112 grams of electrode and 500 mL hydrochloric acid with 500 mL of distilled water.

In this experiment, pre-calcination was utilized to remove graphite from LIBs electrode materials using a muffle and ash furnace at varying temperatures above 700

°C for a period of 2 hours. 30 grams of the electrode material were placed in a ceramic crucible and heated in the muffle furnace to a temperature of 700 °C for 2 hours.

Place	Temperature
Inner furnace	750 °C
Crucible surface	780 °C
Crucible inner side	850 °C

Figure 5.4 : Crucible in Muffle furnace at the temperature of 700 and actual temperatures measured with a heat gun detector.

The resulting calcined sample weighed 22.1 grams, indicating a loss of 8 grams of graphite during the roasting process. XRD analysis was performed on a portion of the calcined sample. 18 grams of the calcined sample were then heated in an ash furnace at 1000 °C for an additional 2 hours, with no significant weight loss observed. Subsequently, the sample was heated to 1150 °C for 1 hour, with no observed change in weight compared to the sample roasted at 700 °C.

Figure 5.5 : Roasting the sample at 1000 °C in an Ash furnace for 2 hours.

Figure 5.6 : Calcined sample after cooling off.

An experiment was conducted to examine the weight loss of a sample resulting from roasting in a muffle furnace at 700 °C and indirect calcination at a temperature that was linearly increased from 1000 to 1150 °C. A ceramic crucible containing 30 grams of electrode material obtained from torn apart lithium-ion batteries (LIBs) was placed in an ash furnace and heated for 2 hours at 1150 °C. The resulting calcined sample weighed 20.6 grams, indicating a reduction of approximately 10 grams of coated graphite during the 2-hour roasting process. The roasted electrodes were subsequently ground to obtain a finer sample for X-ray diffraction analysis. Despite the high temperature and prolonged duration of the experiment, no smelting was observed due to the presence of Mn in the electrodes. A subsequent experiment was conducted at an even higher temperature and longer duration in the ash furnace. An additional experiment was conducted to observe further changes and achieve smelting of the electrodes following an initial calcination at 1150 °C for 2 hours in an ash furnace. 30 grams of electrode material obtained from torn apart lithium-ion batteries (LIBs) were placed in a ceramic crucible and heated for 3 hours at 1200 °C in the ash furnace. The resulting calcined sample weighed 18.6 grams, indicating a further reduction of approximately 12 grams of coated graphite during the 3-hour roasting process at 1200 °C. This suggests that the carbothermic reduction reaction becomes more pronounced at higher temperatures, leading to a greater weight loss compared to roasting at 1150 °C. Post-experiment examination of the crucible revealed that some parts of the sample were adhered to the inner surface of the crucible due to a lack of flux material, resulting from adhesive interactions between the crucible and heated sample during calcination at 1200 °C.

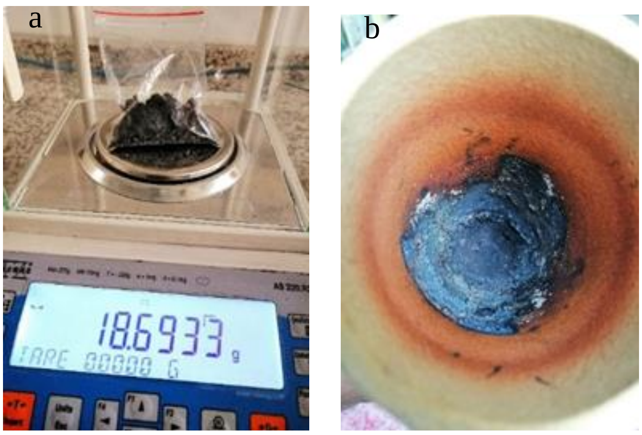

Figure 5.7 : a) Cooled sample at 1200 C for 3 hours, b) top view of the crucible after removal of the roasted sample.

An initial set of results were obtained by smelting at a temperature of 1400 ^{o}C for 30 minutes using 30 grams of electrode material along with a 5% ratio of added flux composed of borax and silica. Experiment 5 involved the testing of three distinct batches, one smelting cathode and anode components separately, one with mixed cathode and anode components, and each with different flux materials, one batch using silica and another using borax. The results indicated that borax was more effective flux compared to silica. The experiment resulted in the expenditure of 13.1 grams of coated graphite during 45 minutes of roasting at 1400 ^{o}C and the formation of a metallic alloy. Following the formation of the metallic alloy, additional experiments were conducted using an induction furnace with the aim of improving the results by addressing certain limitations. The crucible was replaced to prevent any failures during roasting and additional carbon material was added to enhance the carbothermic reduction reaction during the process.

Figure 5.8 : Sample Being Roasted in the Induction furnace at the temprature of 1400 C.

Figure 5.9 : The smelted sample after cooling which the metalic part is located in the middle of the slag.

5.3 Induction Furnace Smelting

In a series of experiments, 60.83 grams of electrode material obtained from two torn apart lithium-ion batteries were placed in a graphite crucible and heated in an induction furnace at a temperature range of 1150-1250 ^{o}C for a period of 5 minutes. The characteristics of the batteries are detailed in a accompanying table 5.2. The resulting output was cast into a mold and separated through a mesh to distinguish the slag, ash, and metallic portions. The first experiment involved the inclusion of a 5% carbon addition to the mixed material. The outcome was 7.6 grams of fine dust, 18.18 grams of metallic residue, and slag.

Table 5.2 : Mixed electrode with cathode and anode.

Part	Unit	Weight (g)	Weight (g)	Total (%)	
		Battery 1	Battery 2		
LIB	2	32.61	34.22	66.83	
Aluminum covers	2	6.99 – 7.01	6.79 - 6.81	13.81	20.66
Plastic isolators	2	1.75 – 1.83	2.22 – 2.32	4.15	6.2
Electrode material	2	Cathode 13.85	13.74	27.59	41.28
		Anode 7.63	7.92	15.55	23.27
Headers	2	0.29 – 0.31	0.32	0.63	0.95
Carbon addition	-	-		5	10

5.4 Induction Furnace Experiments

In a subsequent set of experiments using induction furnace smelting, 67.64 grams of electrode material obtained from two torn apart lithium-ion batteries were placed in a graphite crucible and heated in an induction furnace at a temperature range of 12000-1250 ^{o}C for a period of 5 minutes. The characteristics of the batteries are detailed in a accompanying table 5.3. A mixture of flux materials, 2.27 grams of Borax, 2.27 grams of Silica and 4.54 grams of Sodium carbonate were added to the system prior to smelting. The resulting output was cast into a mold and separated through a mesh to distinguish the slag, ash, and metallic portions. The outcome was 13.59 grams of ash mixed with metallic fine grains, 19.59 grams of metallic residue, and slag.

Table 5.3 : Mixed Electrode with cathode and anode and flux.

Flux	Weight (g)	Part	Unit	Weight (g)		Weight (g)	Total (%)	
				Battery 1		Battery 2		
Borax	2.27	LIB	2	34.82		32.82	67.64	
Silica	2.27	Aluminum covers	2	7.24 – 7.26		7	14.26	21.09
Sodium Carbonate	4.54	Plastic isolators	2	1.54		1.97	3.51	5.2
		Electrode material	2	Cathode	15.11	13.50	28.61	42.29
				Anode	8.95	7.91	16.86	24.92
		Headers	2	0.36		0.34	0.7	1.03

In a further set of experiments, 69.08 grams of electrode material obtained from two torn apart lithium-ion batteries were placed in a graphite crucible and heated in an induction furnace at a temperature range of 1250-1300 °C for a period of 5 minutes. The characteristics of the batteries are detailed in an accompanying table 5.4. A mixture of flux materials, 2.32 grams of Borax, 4.5 grams of Silica, 4.4 grams of Sodium carbonate, and an additional 8.8 grams of carbon were added to the system prior to smelting. The resulting output was cast into a mold and separated through a mesh to distinguish the slag, ash, and metallic portions. The outcome was 14.55 grams of ash mixed with coarser dust, 23.66 grams of metallic residue, and slag.

Table 5.4 : Mixed Electrode with cathod and anode with added flux and carbon.

Flux	Weight	Part	Unit	Weight (g)		Weight (g)	Total	
				Battery 1		Battery 2		
Borax	2.32	LIB	2	35.87		33.21	69.08	
Silica	4.5	Aluminum covers	2	7.26		6.73	13.99	20.25
Sodium Carbonate	4.4	Plastic isolators	2	1.87		2.22	4.09	5.92
Carbon	8.8	Electrode material	2	Cathode	15.25	13.7	28.95	41.9
				Anode	8.62	7.65	16.27	23.55
		Headers	2	0.37		0.34	0.71	1.02

In the following series of experiments, an effort was made to elaborate on previous experimentation by smelting the anode and cathode portions of the lithium-ion batteries separately. Different mixtures were added to the separated electrodes. 103.51 grams of electrode material obtained from three torn apart lithium-ion batteries were placed in two graphite crucibles and heated in an induction furnace at two temperature ranges, 1200-1300 ^{o}C, for a period of 5 minutes. The characteristics of the batteries are detailed in an accompanying table 5.5. In this experiment, a mixture of flux materials, along with a carbon addition, were added to the test electrodes in two distinct experiments. The first batch comprised of only anode material, 25.67 grams, with added flux, the composition of which is detailed in a accompanying table 5.5. The anode component was smelted at a temperature of 1200 ^{o}C, resulting in an output of 6.85 grams of metallic balls, and 17.85 grams of ash. The second batch comprised of only cathode material, 43.54 grams, with added flux and carbon, the composition of which is detailed in a accompanying table 5.5. The cathode component was smelted at a temperature of 1300 ^{o}C, resulting in an output of 28.73 grams of metallic and slag, and 7.3 grams of ash.

Table 5.5 : Seperated Electrode with cathod and anode with added flux and carbon.

Part	Unit	Weight (g)		Weight (g)	Weight (g)	Total (%)	
		Battery 1		Battery 2	Battery 3		
LIB	3	35.41		35.14	32.96	103.51	
Aluminum covers	3	7.41		7.25	6.43	21.09	20.37
Plastic isolators	3	1.65		1.71	2.37	5.73	5.53
Electrode material	3	Cathode	15.05	15.11	13.38	43.54	42.06
		Anode	8.81	8.62	8.24	25.67	24.79
Headers	3	0.28		0.31	0.42	1.01	0.97

Table 5.6 : Added Flux to the Cathode and anode samples.

Cathode		Anode	
Flux	Weight (g)	Flux	Weight (g)
Borax	1.13	Borax	2.15
Silica	1.13	Silica	2.15
Sodium carbonate	2.23	Sodium carbonate	4.3
Carbon	-	Carbon	8.46

After observing the conditions applied regarding the induction purpose the best criteria was selected and further 4 experiments were partaken to try to optimize and maximize the selected smelting process. The initial sample underwent a smelting process at a predetermined temperature range of 1350 – 1400 °C, predicated on the flux ratio derived from the ninth experiment, accompanied by a 15% carbon supplement. Subsequent trials also utilized the same temperature range but introduced variations in the carbon supplement and its typology to optimize the carbon reduction reaction. The secondary trial incorporated a 50% carbon supplement for the anode material and 40% for the cathode material. In the ensuing experiment, the carbon supplement was escalated to 100% for anode electrodes and 60% for cathode electrodes. The input material for the cathode consisted of 94 grams of shredded sheets in conjunction with the flux and supplementary carbon. The resultant output weighed 148 grams, reflecting a weight reduction of 50 grams indicative of the carbothermic reduction reaction. The

metallic

portion of the sample weighed 65 grams.

Table 5.7 : Break Down of last 4 selected induction smelting experiments.

Product	Battery Weight (g)	Electrode Weight (g)	Temperature (C°)	Metal XRF Elements				Flux (g)		Added Carbon (g)	
				Mn	Ni	Co	Cu	SiO_2	Na_2CO_3	$Na_2[B_4O_5(OH)_4]\cdot 8H_2O$	C
1	C	128.1	1250-1300	96.24	0.369	1.22	0.202	12.81	12.81	6.4	19.2
	A	74.5	1250-1300	1.48	0.244	0.679	93.03	7.45	7.45	3.77	11.4
After induction smelting anode grain = 10.6g ash = 66.9gram cathode 138.9											
2	C	90	1250-1300	39.4	0.46	53.26	5.76	9	9	4.5	36
	A	55	1250-1300	5.05	-	1.44	89.23	5.5	5.5	2.75	27.5
After induction smelting anode grain = 33g ash = 22.4gram cathode finer: 5.5g coarse:63g 50% and 40% carbon addition											
3	C	94	1250-1300	92.04	-	1.64	0.978	9.4	9.4	4.8	70.5
	A	60	1250-1300	1.18	-	0.629	91.73	6	6	3	75
After induction smelting anode = 78.8 cathode: 148.6 100% and 60% carbon addition (stoichiometric)											
4	A	50	1250-1350	3.17	-	1.14	89.3	-	5	2.5	50

The sample's elemental composition was as follows: 95% Mn, 2% Cu, 2% Co, and 1% Ni. Recovery rates for these elements in their metallic forms, as calculated from Table 5.6, are as follows: 65% for Mn, 52% for Co, and 69% for Ni.

Table 5.8 : Cathode XRF analysis for the sample with 50% carbon addition.

Product		Electrode Weight (g)	Temperature (C^o)	Metal XRF Elements				Flux (g)		Added Carbon (g)	
				Mn	Ni	Co	Cu	SiO_2	Na_2CO_3	$Na_2 [B_4 O_5 (OH)_4] \cdot 8 H_2O$	C
9	C	93	1350-1400	89.7	4.02	2.79	2.27	9.3	9.3	4.7	46.5

For process confirmation another experiment was taken regarding cathode smelting output of the experiment was divide in 3 categories which were a big portion of solid metallic, small coarse and ash portion.

Table 5.9 : Weight ratio from XRF analysis of experimented Sample.

	Total weight	Mn (g)	Mn (%)	Ni (g)	Ni (%)	Co (g)	Co (%)	Cu (g)	Cu (%)
Solid Metallic	32	24	75	2.6	8.12	1.6	5	2.4	7.5
Small Coarse metals	43	39	90.6	1	2.32	1	2.32	2	4.6
Ash	18	16	88.8	0.62	4.12	0.38	2.1	1	5.5

It is observed that the recovery rate of Mn in the metallic portion is 75% that is a highlight regarding the extraction.

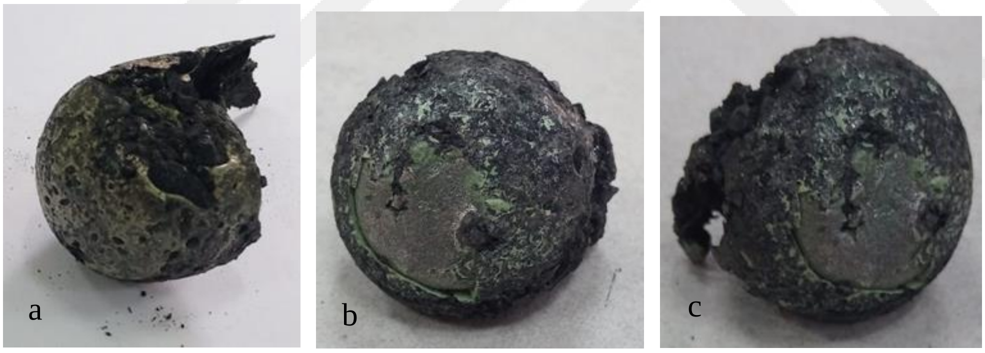

Figure 5.10 : The Output of induction furnace with a) 45% b) 50% c) 60% carbon addition along with added flux material.

6. RESULTS AND DISCUSSION

In this chapter, the discussion and results of the recovery of valuable metals from waste lithium-ion batteries by metallurgical routes are presented. The experiments were divided into two batches, with the first batch focusing on pyrometallurgical roasting and smelting without added flux. The second batch of experiments were carried out in an induction furnace and included the use of flux and carbon addition. The results of these experiments will be analyzed and discussed in detail, providing insight into the effectiveness of different metallurgical routes for recovering valuable metals from waste lithium-ion batteries. The overall aim of this research is to develop cost-effective and environmentally friendly methods for recovering valuable metals from waste lithium-ion batteries, and this chapter will provide a comprehensive overview of the progress made towards this goal.

6.1 Results and Discussion of Calcination and Smelting of Samples through Ash Furnace and Muffle Furnace

In this experiment, 20 units of waste lithium-ion batteries (LIBs) with a total weight of 692.9 grams were disassembled and separated from their casings. The individual parts were weighed for accurate calculations. A portion of the electrode material, specifically 112.3 grams, was taken from the LIBs and placed in a beaker. This material was then leached in a solution of Hydrochloric acid (50%wt) and distilled water (50%wt) for a duration of 2 hours at an average temperature of 85.5 ^{o}C.

Three samples of 50 ml were taken from the heated leached solution at 30 minutes, 1 hour, and 2 hours for chemical analysis. The first two samples taken at 30 minutes and 1 hour were taken out with a dropper and transferred to small beakers for examination. However, the last sample taken at 2 hours was considered to give more accurate results, so the heating process was stopped after 2 hours, filtered, and the solid cake containing the electrodes was separated and dried in an oven for 12 hours. This solid cake was also sent for separate chemical analysis. The samples taken from the leached solution were filtered using mesh papers and a strainer to obtain a clearer leach solution and remove any large particles before sending them for chemical analysis. The sample solutions that were taken at min 30, 60, and 120 were sent for Atomic absorption spectrometry, which the results are given as follows.

Figure 6.1 : 10 mL sample solutions of minutes 30, 60 and 120 taken from the HCl solution

6.2 Atomic Absorption Spectrometry (AAS)

Table 6.1 : AAS analysis of the leached cake with different diluting factor.

Co		Cu		Ni		Mn		Li	
Sample	Result (mg/L)	Sample	Result (mg/L)	Sample	Result (mg/L)	Sample	Result (mg/L)	Sample	Result (mg/L)
30 min	0,393	30 min	0,245	30 min	1,819	30 min	0,766	30 min	0,843
60 min	0,686	60 min	0,542	60 min	3,054	60 min	1,460	60 min	1,210
2h	0,914	2h	0,771	2h	5,574	2h	2,399	2h	2,024

**Co: (dilution factor =500); Cu: (dilution factor =5000); Ni: (dilution factor =50); Mn: (dilution factor =5000); Li: (dilution factor =500)

In summary, based on our findings, the primary constituents discerned in the discarded lithium-ion batteries (LIBs) comprise Manganese (Mn), Cobalt (Co), Nickel (Ni), and Copper (Cu). For a heightened degree of accuracy, we propose undertaking a more extensive investigation through the application of Atomic Absorption Spectroscopy (AAS) on the pertinent sample solutions in subsequent research endeavors. The implementation of this analytical technique will be instrumental in ascertaining the most cost-effective methodology for the extraction of precious metals from LIBs, which stands as the primary objective of the present study. For the second experiment, a pre pyro metallurgical path was selected to remove the coated graphite on the copper sheets before continuing with the hydrometallurgical leaching.

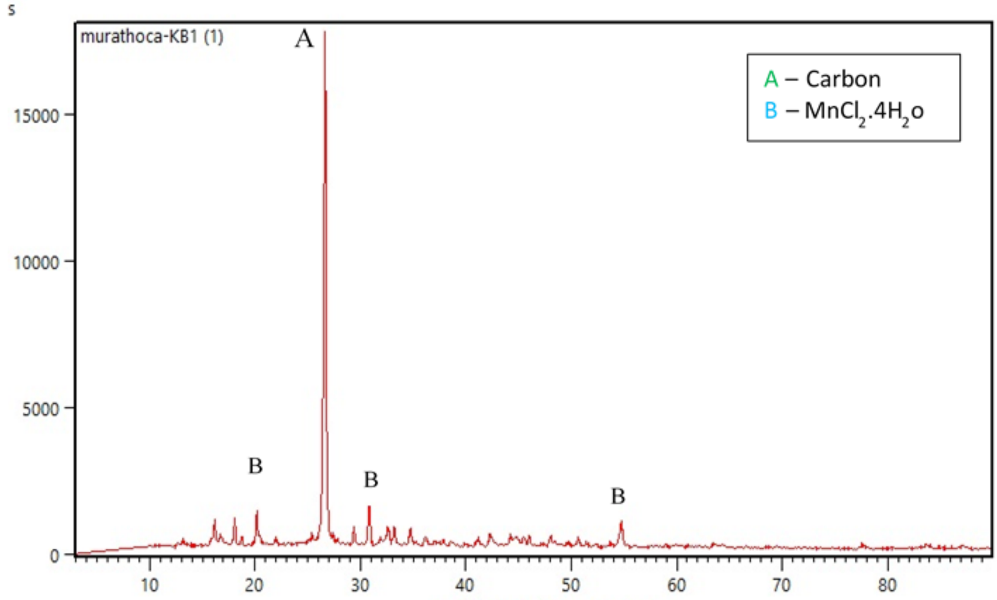

Figure 6.2 : Dried leached cake XRD analysis.

6.3 XRD Analysis of The Leched Cake of Smelted Samples in the Muffle Furnace

Following the leaching process, the resulting cake was dried for 12 hours and subsequently weighed. The dried cake was then subjected to mill grinding for a duration of 5 minutes in order to obtain a finer material for X-ray Diffraction (XRD) analysis. Following the grinding process, pure copper sheets that were not ground were separated and the remainder of the sample was weighed and prepared for further analysis. Through the mechanical separation of the lithium-ion batteries (LIBs), two parts of the LIBs were selected for analysis, one for X-ray Fluorescence (XRF) analysis of the aluminum casing and the other for structural analysis of the LIB isolators through Fourier Transform Infrared Spectroscopy (FT-IR). The primary element identified in the leached cake as seen from the Figure 6.2 was carbon as it was expected. Further processes will be conducted on the remaining elements present in the solution.

6.4 XRD Analysis of The Indirect Calcination

In this study, an electrode material taken from disassembled lithium-ion batteries (LIBs) with a mass of 30 grams was placed in a ceramic crucible and placed in a muffle furnace. The furnace was heated for 3 hours to reach the target temperature. The sample was subsequently subjected to calcination for a period of 2 hours within the furnace, with an inner temperature of 850 °C and a surface temperature of 780 °C. 3 grams of the calcined sample were extracted for X-ray Diffraction (XRD) analysis. A portion of pure copper that remained in the roasted sample was separated and the remaining 18 grams were further roasted in an ash furnace at a temperature of 1000 °C for 2 hours. Following the roasting process, the sample was cooled and weighed. It was observed that there was minimal change in weight loss. 3 grams of the roasted sample at 1000 °C were sent for XRD analysis. The next step was to heat the sample to 1150 °C to monitor weight change and investigate if the excess graphite would be eliminated, allowing for a finer sample for hydrometallurgical leaching to enhance the recovery of valuable metals such as cobalt and copper. The XRD analysis in Figure 6.3 revealed that cobalt was the primary element found in the smelted sample, which was the result of the further roasting in the ash furnace.

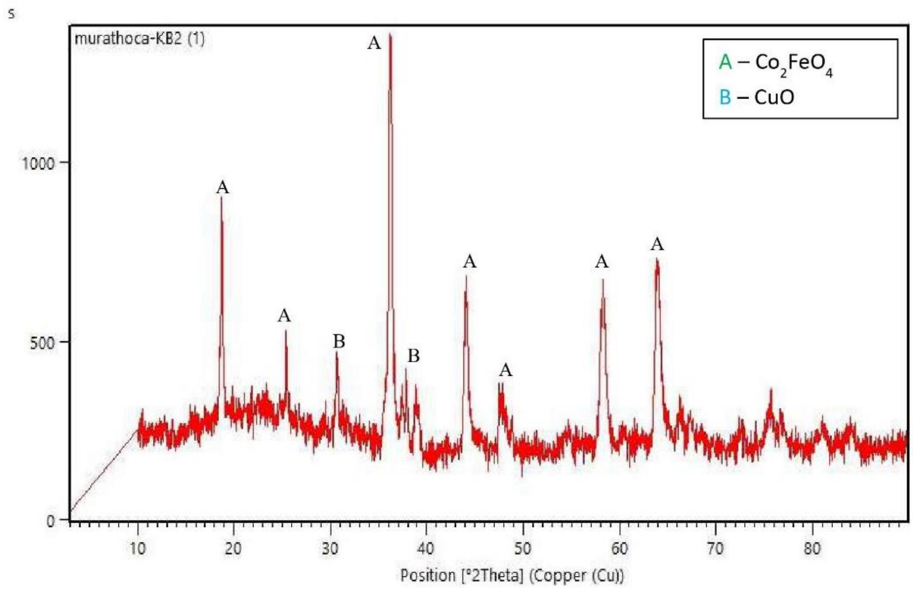

Figure 6.3 : XRD analysis of indirect calcination from 700 to 1150 °C.

6.5 XRD Analysis of The direct Calcination

This experiment was conducted after observing no significant change in weight loss for the sample that was subjected to roasting at 700 °C in a muffle furnace, following the indirect calcination process at a temperature that was incrementally increased from 1000 to 1150 °C. The roasted electrodes were then ground to obtain a finer sample for X-ray Diffraction (XRD) analysis. It is important to note that the XRD analysis can provide information about the crystal structure and phase composition of the sample, and can be a useful tool in identifying the presence of valuable metals such as cobalt and copper. Additionally, the grinding process can improve the surface area of the sample and enhance the leaching efficiency of the hydrometallurgical process that follows.

As can be inferred from the X-ray Diffraction (XRD) analysis conducted on the sample obtained from direct calcination, the main present elements are depicted in the figure 6.4 below. This XRD analysis can provide information on the crystal structure and phase composition of the sample and can be useful in identifying the presence of valuable metals such as cobalt and copper. Furthermore, the results of this analysis can be used to understand the effects of direct calcination on the sample and to guide further research and experimentation towards the recovery of valuable metals from lithium-ion batteries (LIBs).

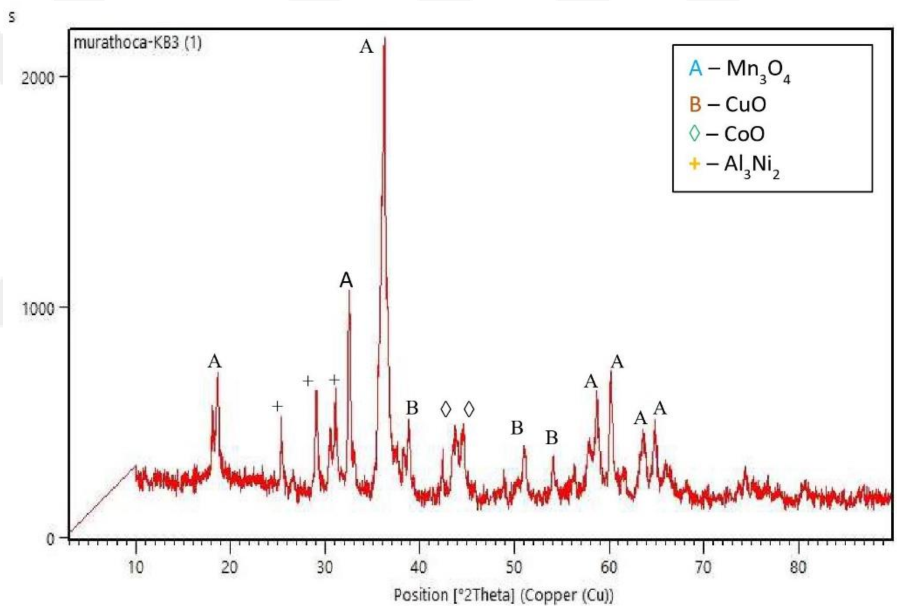

Figure 6.4 : XRD analysis of direct calcination of 30 grams electrode at 1200 ^{o}C.

6.6 XRD Analysis of The Raw and Smelted Anode Sheets and Induction Furnace Output

After several experiments regarding the pyrometallurgical routes for anode electroes that there elemental composition is 99 percent Copper, we smelted the last sample with a 100% stoichiometric carbon addition (Carbon Black) and the output and the raw material were sent for XRD analysis.

Anode is mostly made of carbon and little amount of copper and copper oxide Raw material is made of copper and carbon, but this has more copper than anode. Through the course of several rigorous experimental processes, we have investigated the pyrometallurgical pathways applicable to anode electrodes, which consist primarily of elemental Copper with a composition of approximately 99%.

Our most recent trial involved the smelting of a sample with a 100% stoichiometric addition of Carbon Black, a variant of amorphous carbon recognized for its high surface area to volume ratio.

Following this smelting procedure, both the resultant output and the raw material were subjected to X-ray Diffraction (XRD) analysis, a powerful tool for elucidating the crystallographic structure, chemical composition, and physical properties of materials. XRD analysis allowed us to accurately determine and quantify the constituents of the sample.

The anode under examination was found to be largely composed of carbon, with only a minimal amount of copper and copper oxide interspersed within its matrix. This composition highlights the essential role carbon plays in facilitating electron transfer within the battery's electrochemical reactions.

Conversely, the raw material used, characterized by a combination of copper and carbon, was discerned to contain a significantly higher copper content compared to that in the anode. The preponderance of copper in this context is likely attributable to its superior electrical conductivity, which plays a pivotal role in efficient energy transfer. Through these experimental findings, we seek to augment our understanding of the pyrometallurgical processes related to anode electrodes and contribute valuable insights that may inform the design and fabrication of more efficient and sustainable energy storage systems.

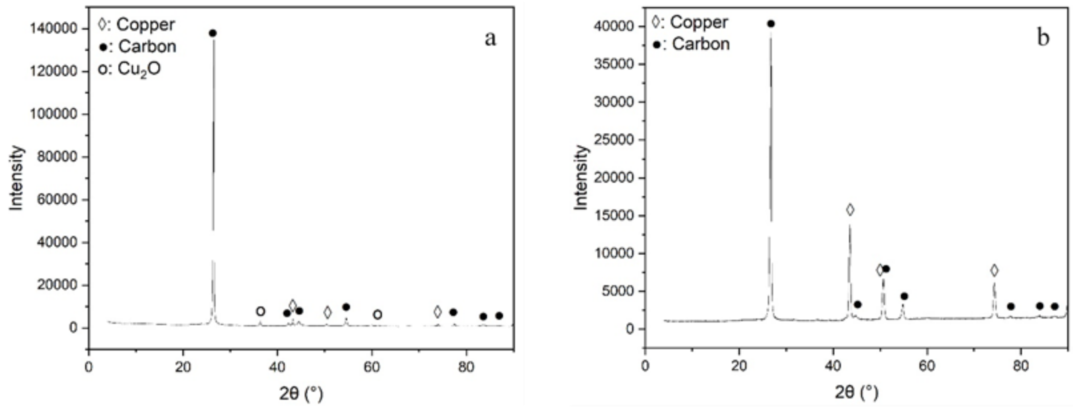

Figure 6.5 : XRD analysis of anode electrodes a) Smelted sample with carbon balck b) Raw anode sheets taken from seperated LIB and grinded.

6.7 Induction Furnace Smelting Discussion and Results

During the span of our investigative study, we conducted a sequence of methodical trials with the objective of extracting materials from lithium-ion batteries in a manner congruent with environmental sustainability. In the inaugural experimental series, a smelting process was employed. This involved the use of electrode materials, subjected to a temperature of 1400 ^{o}C for a period of 30 minutes, and the introduction of a flux mixture comprised of 5% borax and silica. Our investigation encompassed three distinct experimental batches: one where the cathode and anode constituents were smelted in isolation, another wherein they were co-smelted, and a third that employed an alternative flux mixture of silica and borax. The observations from this stage indicated a superior efficacy of borax over silica in the formation of a metallic alloy. Subsequent to these initial trials, we proceeded with an examination employing an induction furnace. This step was designed to rectify some of the constraints identified in the preliminary experiments. Enhancements were implemented through the introduction of carbon to the sample, thereby bolstering the carbothermic reduction reaction during the procedure. The ensuing set of trials utilized 60.83 grams of assorted electrode material, sourced from deconstructed LIBs. These were placed in a graphite crucible and roasted within a temperature interval of 1150-1250 ^{o}C for a duration of 5 minutes. The resultant output included 7.6 grams of fine particulate matter, 18.18 grams of metallic residues, and additional slag.

Furthering our investigation, we implemented a second series of induction furnace smelting trials. Herein, we utilized 67.64 grams of assorted electrode material, with the inclusion of a flux mixture constituting 2.27 grams each of borax and silica, alongside 4.54 grams of sodium carbonate. The product of this experimental sequence comprised 13.59 grams of ash intermingled with fine metallic grains, and 19.59 grams of metallic remnants, in addition to slag. This progression of methodically conducted experiments further deepens our understanding of the sustainable extraction of valuable materials from lithium-ion batteries.

In the third sequential set of trials, we modified the isolated electrodes with the integration of both carbon and flux. The experiment utilized 69.08 grams of electrode material and introduced a flux mixture consisting of 2.32 grams of borax, 4.5 grams of silica, 4.4 grams of sodium carbonate, and an additional allotment of 8.8 grams of carbon. The resultant output yielded 14.55 grams of ash commingled with coarse dust, along with 23.66 grams of remaining metallic constituents in addition to slag.

In the subsequent series, our objective was to build upon preceding endeavors by smelting the anode and cathode components of the lithium-ion batteries (LIBs) independently. We employed 103.51 grams of electrode material derived from three disassembled LIBs, which were allocated into graphite crucibles and subjected to a temperature spectrum of 1200-1300 ^{o}C for a span of 5 minutes. Concurrently, we incorporated a diverse assortment of flux materials and carbon additions to the electrodes. The data extracted from these trials have been cataloged in the table 6.1.

The inaugural sample was subjected to smelting within the predetermined temperature bracket of 1350 – 1400 °C. The selection of this temperature range was informed by the flux ratio discerned from the ninth experiment, and supplemented with a 15% carbon addition. Subsequent trials adhered to this temperature range while varying the proportion and nature of the carbon supplement to optimize the carbon reduction reaction.

In the ensuing trials, the carbon supplement was increased to 50% for the anode material and 40% for the cathode material. The subsequent trial elevated the carbon addition to 100% for anode electrodes and 60% for cathode electrodes. The cathode's input material consisted of 94 grams of shredded sheets, augmented with flux and additional carbon. The output weighed 148 grams, reflecting a 50-gram reduction in weight indicative of the carbothermic reduction reaction. The metallic fraction of the sample weighed 65 grams.

The predominant elemental composition of the sample included Manganese (Mn) at 95%, Copper (Cu) at 2%, Cobalt (Co) at 2%, and Nickel (Ni) at 1%. The recovery rates of these elements in their metallic form, as extrapolated from Table 5.9 (previous chapter), were: Mn at 65%, Co at 52%, and Ni at 69%. To validate the procedure, an additional trial focusing on cathode smelting was performed. The experimental output was segmented into a considerable solid metallic fraction, a minor coarse fraction, and an ash fraction. A salient observation was the recovery rate of Mn in the metallic fraction, which registered at 75%, highlighting the efficiency of the extraction procedure.

Overall, the outcomes of these experimental iterations indicate that the integration of borax as a flux material and the inclusion of carbon may ameliorate the environmentally-conscious extraction of materials from lithium-ion batteries. However, to refine the process and amplify the recovery rate of valuable metals, additional research and systematic experimentation are necessitated.

Table 6.2 : Comparison of different pathways of smelting for recovery of valuable metals from LIBs.

Experiment	Battery Weight (g)	Electrode Weight (g)	Temperature (C°)	Metal XRF Elements				Added Flux (g)		Added Carbon (g)	
				Mn	Ni	Co	Cu	SiO_2	Na_2CO_3	$Na_2[B_4O_5(OH)_4]\cdot 8H_2O$	C
1	66.83	43.04	1150-1250	63.95	0.208	0.777	34.98	-	-	-	5
2	67.64	45.47	1200-1250	62.4	2.46	1.36	33.6	2.27	4.54	2.27	-
3	69.08	45.22	1250-1300	70.2	2.34	1.86	24.5	4.5	4.4	2.32	8.8
4	103.51	A 25.67	1200-1300	43.1	1.78	0.66	54.1	1.13	2.23	1.13	-
5	103.51	C 43.54	1300	-	-	-	-	2.15	4.3	2.15	8.46
6	69.54	44.74	1250-1300	52.7	2,56	0.71	43.5	4.5	4.5	2.25	8.94
7	71.34	47.8	1250-1300	59.0	3.46	1.86	28.8	5	5	2.5	11.95
8	72.21	48.43	1250-1300	-	-	-	-	5	5	2.5	14.55
9	**105.45**	**C 43.77**	**1250-1300**	**89.7**	**4.02**	**2.79**	**2.27**	**4.3**	**4.3**	**2.15**	**6.56**
		A 25.03						**2.5**	**2.5**	**1.25**	**3.75**
10	**105.12**	**C 42.35**	**1250-1300**	**90.5**	**2.06**	**1.84**	**1.42**	**4.2**	**4.2**	**2.1**	**6.35**
		A 23.09		**29.7**	**0.44**	**0.27**	**59.6**	**2.3**	**2.3**	**1.15**	**3.45**
11		C 128.1	1250-1300	96.24	0.369	1.22	0.202	12.81	12.81	6.4	19.2
		A 74.5	1250-1300	1.48	0.244	0.679	93.03	7.45	7.45	3.77	11.4
After induction smelting anode grain = 10.6g ash = 66.9-gram cathode 138.9											
12		C 90	1250-1300	39.4	0.46	53.26	5.76	9	9	4.5	36
		A 55	1250-1300	5.05	-	1.44	89.23	5.5	5.5	2.75	27.5
After induction smelting anode grain = 33g ash = 22.4-gram cathode finer: 5.5g coarse:63g 50% and 40% carbon addition											
13		C 94	1250-1300	92.04	-	1.64	0.978	9.4	9.4	4.8	70.5
		A 60	1250-1300	1.18	-	0.629	91.73	6	6	3	75
After induction smelting anode = 78.8 cathode: 148.6 100% and 60% carbon addition (stoichiometric)											
14		A 50	1250-1350	3.17	-	1.14	89.3	-	5	2.5	50
Smelting in induction furnace without any added silica along with 100 % carbon addition (carbon black) – result: 82 grams as ash											

7. CONCLUSIONS AND RECOMMENDATIONS

In conclusion, the research presented in this thesis aimed to recover valuable metals from waste lithium-ion batteries through metallurgical routes. The experiments were conducted in several stages, including leaching, roasting, and smelting. The results of the experiments showed that the use of borax as a flux material and the addition of carbon material can enhance the extraction of valuable metals in an environmentally friendly manner.

In the leaching experiment, a quarter of the electrode material was placed in a Hydrochloric acid solution for 2 hours, and samples were taken at various intervals for chemical analysis. The results showed that the main element in the leached solution was copper, with other valuable metals present in smaller quantities.

The calcination and roasting experiments were conducted in a muffle furnace and an ash furnace, respectively. The results of the X-ray diffraction (XRD) analysis showed that the main element in the roasted samples was cobalt, with other valuable metals present in smaller quantities. The samples were further roasted at higher temperatures to improve the recovery rate of valuable metals.

The smelting experiments were conducted at a temperature of 1400 ^{o}C for 30 minutes, using a 5% ratio of added flux including borax and silica. The results showed that silica was not as effective as borax in achieving a metallic alloy. A series of experiments under an induction furnace were also conducted to improve the accuracy of the results by addressing some drawbacks from the previous experiment. The results of the experiments showed that the use of borax as a flux material and the addition of carbon material can enhance the extraction of lithium-ion batteries in an environmentally friendly manner.

Overall, the results of the experiments show that metallurgical routes can be an effective way to recover valuable metals from waste lithium-ion batteries. However, further research and experimentation are needed to optimize the process and improve the recovery rate of valuable metals. Some potential areas of future research include the optimization of leaching conditions, the use of different roasting and smelting techniques, and the development of more efficient methods for separating and recovering valuable metals.

One future direction of research could be focused on developing a more efficient hydrometallurgical process for the recovery of valuable metals from the leached solution. Currently, the recovery rate of valuable metals such as cobalt and copper is relatively low, and there is potential to improve this through the development of new leaching agents or optimizing existing ones. Additionally, the use of advanced techniques such as solvent extraction or ion exchange could further improve the recovery rate of valuable metals.

Another area of research could be focused on developing an environmentally friendly direct smelting process for the recovery of valuable metals from waste lithium-ion batteries. Currently, the direct smelting process generates a significant amount of emissions, including greenhouse gases and pollutants, which can have negative impacts on the environment. Developing new technologies, such as the use of alternative energy sources or carbon capture and storage, could help to mitigate these environmental impacts and make the process more sustainable.

In addition to these technological advancements, further research is needed to understand the environmental impacts of lithium-ion battery recycling and to identify pathways for the responsible disposal of waste lithium-ion batteries. This research could focus on understanding the environmental impacts of different recycling processes, such as the leaching of valuable metals, the generation of emissions during direct smelting, and the disposal of waste materials after the recovery of valuable metals.

Finally, it is important to note that recycling lithium-ion batteries is just one aspect of the larger challenge of dealing with e-waste. Therefore, it is essential to consider the entire life cycle of lithium-ion batteries and to identify ways to reduce the environmental impacts of their production, use, and disposal. This could include encouraging the use of more sustainable materials in the production of lithium-ion batteries, designing products for longevity and repairability, and promoting the circular economy through the reuse and refurbishment of lithium-ion batteries.

In summary, the metallurgical recovery of valuable metals from waste lithium-ion batteries is a promising approach to dealing with e-waste. However, further research is needed to optimize the process and minimize the environmental impacts of recycling. Advances in hydrometallurgical techniques, direct smelting processes, and understanding of the environmental impacts of lithium-ion battery recycling are all important areas for future research. Additionally, a comprehensive approach that considers the entire life cycle of lithium-ion batteries and promotes sustainable practices is needed to address the growing problem of e-waste.

REFERENCES

[1] **J. Choi, P.J. Kim,** (2022) A roadmap of battery separator development: Past and future, Curr. Opin. Electrochem. 31 1–9. https://doi.org/10.1016/j.coelec.2021.100858.

[2] **R. Danino-Perraud,** The Recycling of liThium-ion BaTTeRies A Strategic Pillar for the European Battery Alliance études de l'Ifri Raphaël Danino-PeRRauD Center for Energy, 2020.

[3] **IEA, Global EV Outlook** (2022) - Securing supplies for an electric future, Glob. EV Outlook 2022. (2022) 221. https://www.iea.org/reports/global-ev-outlook-2022%0Ahttps://iea.blob.core.windows.net/assets/ad8fb04c-4f75-42fc-973a-6e54c8a4449a / GlobalElectric Vehicle Outlook 2022. pdf.

[4] **W. Mrozik, M.A. Rajaeifar, O. Heidrich, P. Christensen,** Environmental impacts, pollution sources and pathways of spent lithium-ion batteries, Energy Environ. Sci. 14 (2021) 6099–6121. https://doi.org/10.1039/d1ee00691f.

[5] **B. Balasubramaniam, N. Singh, S. Verma, R.K. Gupta,** Recycling of Lithium From Li-ion Batteries, Encycl. Renew. Sustain. Mater. (2020) 546–554. https://doi.org/10.1016/b978-0-12-803581-8.10764-7.

[6] **A. Holzer, L. Wiszniewski, S. Windisch-Kern, H. Raupenstrauch,** Optimization of a Pyrometallurgical Process to Efficiently Recover Valuable Metals from Commercially Used Lithium-Ion Battery Cathode Materials LCO, NCA, NMC622, and LFP, Metals (Basel). 12 (2022). https://doi.org/10.3390/met12101642.

[7] **M. Wakihara,** Recent developments in lithium ion batteries, Mater. Sci. Eng. R Reports. 33 (2001) 109–134. https://doi.org/10.1016/S0927-796X(01)00030-4.

[8] **S. S. Rangarajan, S.P. Sunddararaj, A. Sudhakar, C.K. Shiva, U. Subramaniam, E.R. Collins, T. Senjyu,** Lithium-Ion Batteries—The Crux of Electric Vehicles with Opportunities and Challenges, Clean Technol. 4 (2022) 908–930. https://doi.org/10.3390/cleantechnol 4040056.

[9] **M. Chen, X. Ma, B. Chen, R. Arsenault, P. Karlson, N. Simon, Y. Wang,** Recycling End-of-Life Electric Vehicle Lithium-Ion Batteries, Joule. 3 (2019) 2622–2646. https://doi.org/10.1016/j.joule.2019.09.014.

[10] **E. Mossali, N. Picone, L. Gentilini, O. Rodrìguez, J.M. Pérez, M. Colledani,** Lithium-ion batteries towards circular economy: A literature review of opportunities and issues of recycling treatments, J. Environ. Manage. 264 (2020). https://doi.org/10.1016/j.jenvman.2020.110500.

[11] **P. Roy, S.K. Srivastava,** Nanostructured anode materials for lithium ion batteries, J. Mater. Chem. A. 3 (2015) 2454–2484. https://doi.org/10.1039/c4ta04980b.

[12] **S.S. Zhang,** The effect of the charging protocol on the cycle life of a Li-ion battery, J. Power Sources. 161 (2006) 1385–1391. https://doi.org/10.1016/j.jpowsour.2006.06.040.

[13] **C.J. Orendorff,** The role of separators in lithium-ion cell safety, Electrochem. Soc. Interface. 21 (2012) 61–65. https://doi.org/10.1149/2.F07122if.

[14] **P. Zhu, D. Gastol, J. Marshall, R. Sommerville, V. Goodship, E. Kendrick,** A review of current collectors for lithium-ion batteries, J. Power Sources. 485 (2021) 229321. https://doi.org/10.1016/j.jpowsour.2020.229321.

[15] **C. Daniel,** Materials and processing for lithium-ion batteries, Jom. 60 (2008) 43–48. https://doi.org/10.1007/s11837-008-0116-x.

[16] **J. Schoonman,** Nanostructured materials in solid state ionics, Solid State Ionics. 135 (2000) 5–19. https://doi.org/10.1016/S0167-2738(00)00324-6.

[17] **Faculty of Engineering Chemical Engineering Department** Aproject Ion Lithium battery Presented By Khalid AbuaqilahMasoud Supervised By, (2019).

[18] **M.S. Whittingham,** See Also Sidebar :, (1967) 411–419.

[19] **C. Daniel,** Lithium ion batteries and their manufacturing challenges, Bridg. (Washington, D.C.). 45 (2015) 21–24.

[20] **A.I. Stan, M. Swierczynski, D.I. Stroe, R. Teodorescu, S.J. Andreasen,** Lithium ion battery chemistries from renewable energy storage to automotive and back-up power applications - An overview, 2014 Int. Conf. Optim. Electr. Electron. Equipment, OPTIM 2014. (2014) 713–720. https://doi.org/10.1109/OPTIM.2014.6850936.

[21] **M. Li, J. Lu, Z. Chen, K. Amine,** 30 Years of Lithium-Ion Batteries, Adv. Mater. 30 (2018) 1–24. https://doi.org/10.1002/adma.201800561.

[22] **M.D. Bhatt, C. O'Dwyer,** Density functional theory calculations for ethylene carbonate-based binary electrolyte mixtures in lithium ion batteries, Curr. Appl. Phys. 14 (2014) 349–354. https://doi.org/10.1016/j.cap.2013.12.010.

[23] **C. Monroe, J. Newman,** The Impact of Elastic Deformation on Deposition Kinetics at Lithium/Polymer Interfaces, J. Electrochem. Soc. 152 (2005) A396. https://doi.org/10.1149/1.1850854.

[24] **X. Huang,** Separator technologies for lithium-ion batteries, J. Solid State Electrochem. 15 (2011) 649–662. https://doi.org/10.1007/s10008-010-1264-9.

[25] **H. Lee, M. Yanilmaz, O. Toprakci, K. Fu, X. Zhang,** A review of recent developments in membrane separators for rechargeable lithium-ion batteries, Energy Environ. Sci. 7 (2014) 3857–3886. https://doi.org/10.1039/c4ee01432d.

[26] **H. Zhang, M.Y. Zhou, C.E. Lin, B.K. Zhu,** Progress in polymeric separators for lithium ion batteries, RSC Adv. 5 (2015) 89848–89860. https://doi.org/10.1039/c5ra14087k.

[27] **P. Arora, Z. Zhang,** Battery separators, Chem. Rev. 104 (2004) 4419–4462. https://doi.org/10.1021/cr020738u.

[28] **M.S. Balogun, Y. Luo, W. Qiu, P. Liu, Y. Tong,** A review of carbon materials and their composites with alloy metals for sodium ion battery anodes, Elsevier Ltd, 2016. https://doi.org/10.1016/j.carbon.2015.09.091.

[29] **Y. Lu, Q. Zhang, J. Chen,** Recent progress on lithium-ion batteries with high electrochemical performance, Sci. China Chem. 62 (2019) 533–548. https://doi.org/10.1007/s11426-018-9410-0.

[30] **F. Schipper, D. Aurbach,** A brief review: Past, present and future of lithium ion batteries, Russ. J. Electrochem. 52 (2016) 1095–1121. https://doi.org/10.1134/S1023193516120120.

[31] **S. Gmar, L. Muhr, F. Lutin, A. Chagnes,** Lithium-Ion Battery Recycling: Metal Recovery from Electrolyte and Cathode Materials by Electrodialysis, Metals (Basel). 12 (2022) 1859. https://doi.org/10.3390/met12111859.

[32] **R. Gao, C. Sun, L. Xu, T. Zhou, L. Zhuang, H. Xie,** Recycling LiNi0.5Co0.2Mn0.3O2 material from spent lithium-ion batteries by oxalate co-precipitation, Vacuum. 173 (2020) 109181. https://doi.org/10.1016/j.vacuum.2020.109181.

[33] **J.J. Roy, S. Madhavi, B. Cao,** Metal extraction from spent lithium-ion batteries (LIBs) at high pulp density by environmentally friendly bioleaching process, J. Clean. Prod. 280 (2021) 124242. https://doi.org/10.1016/j.jclepro.2020.124242.

[34] **Fabiana Meijon Fadul,** 済無No Title No Title No Title, (2019) 1–9.

[35] **Z. Li, A. Li, H. Zhang, F. Ning, W. Li, A. Zangiabadi, Q. Cheng, J.J. Borovilas, Y. Chen, H. Zhang, X. Xiao, C. Ouyang, X. Huang, W.K. Lee, M. Ge, Y.S. Chu, X. Chuan, Y. Yang,** Multi-scale stabilization of high-voltage LiCoO2 enabled by nanoscale solid electrolyte coating, Energy Storage Mater. 29 (2020) 71–77. https://doi.org/10.1016/j.ensm.2020.03.031.

[36] **Y. Dong, P. Su, G. He, H. Zhao, Y. Bai,** Constructing compatible interface between Li7La3Zr2O12solid electrolyte and LiCoO2cathode for stable cycling performances at 4.5 v, Nanoscale. 13 (2021) 7822–7830. https://doi.org/10.1039/d1nr01079d.

[37] **Z. Tianran, L. Daixin, Z. Tao, C. Jun,** Understanding electrode materials of rechargeable lithium batteries via DFT calculations, Prog. Nat. Sci. Mater. Int. 23 (2013) 256–272. https://doi.org/10.1016/j.pnsc.2013.04.005.

[38] **M. Du, Q. Li, H. Pang,** Oxalate-derived porous prismatic nickel/nickel oxide nanocomposites toward lithium-ion battery, J. Colloid Interface Sci. 580 (2020) 614–622. https://doi.org/10.1016/j.jcis.2020.07.009.

[39] **K. Kawashima, T. Ohnishi, K. Takada,** High-Rate Capability of LiCoO2Cathodes, ACS Appl. Energy Mater. 3 (2020) 11803–11810. https://doi.org/10.1021/acsaem.0c01973.

[40] **Y. Mahara, Y. Makimura, H. Oka, H. Nakano, S. Tajima, T. Nonaka, T. Sasaki,** Appearance of the 4 V signal without transformation to spinel-related oxides from loose-crystalline rock-salt LiMnO2, J. Power Sources. 497 (2021) 229788. https://doi.org/10.1016/j.jpowsour.2021.229788.

[41] **Z. Cai, Y. Ma, X. Huang, X. Yan, Z. Yu, S. Zhang, G. Song, Y. Xu, C. Wen, W. Yang,** High electrochemical stability Al-doped spinel LiMn2O4 cathode material for Li-ion batteries, J. Energy Storage. 27 (2020). https://doi.org/10.1016/j.est.2019.101036.

[42] **W. Dong, X. Huang, Y. Jin, M. Xie, W. Zhao, F. Huang,** Building an artificial solid electrolyte interphase on spinel lithium manganate for high performance aqueous lithium-ion batteries, Dalt. Trans. 49 (2020) 8136–8142. https://doi.org/10.1039/d0dt00901f.

[43] **N. Yabuuchi, K. Kubota, M. Dahbi, S. Komaba, N. Yabuuchi, K. Kubota, M. Dahbi, S. Komaba,** Research Development on Sodium-Ion Batteries, Chem. Rev. 114 (2014) 11636-11682, Chem. Rev. 114 (2014) 11636–11682. http://www.ncbi.nlm.nih.gov/pubmed/25390643.

[44] **A. Yamada, S.C. Chung, K. Hinokuma,** Optimized LiFePO[sub 4] for Lithium Battery Cathodes, J. Electrochem. Soc. 148 (2001) A224. https://doi.org/10.1149/1.1348257.

[45] **E. V. Beletskii, E. V. Alekseeva, D. V. Spiridonova, A.N. Yankin, O. V. Levin,** Overcharge cycling effect on the surface layers and crystalline structure of LiFePO4 cathodes of Li-ion batteries, Energies. 12 (2019) 18–21. https://doi.org/10.3390/en12244652.

[46] **X.G. Yang, T. Liu, C.Y. Wang,** Thermally modulated lithium iron phosphate batteries for mass-market electric vehicles, Nat. Energy. 6 (2021) 176–185. https://doi.org/10.1038/s41560-020-00757-7.

[47] **H. Sun, K. Zhao,** Electronic Structure and Comparative Properties of LiNi x Mn y Co z O 2 Cathode Materials , J. Phys. Chem. C. 121 (2017) 6002–6010. https://doi.org/10.1021/acs.jpcc.7b00810.

[48] **W. Yan, S. Yang, Y. Huang, Y. Yang, Guohui Yuan,** A review on doping/coating of nickel-rich cathode materials for lithium-ion batteries, J. Alloys Compd. 819 (2020) 153048. https://doi.org/10.1016/j.jallcom.2019.153048.

[49] **L. Fan, X. Guo, X. Hang, H. Pang,** Synthesis of truncated octahedral zinc-doped manganese hexacyanoferrates and low-temperature calcination activation for lithium-ion battery, J. Colloid Interface Sci. 607 (2022) 1898–1907. https://doi.org/10.1016/j.jcis.2021.10.025.

[50] **S. Watanabe, M. Kinoshita, K. Nakura,** Capacity fade of LiNi(1-x-y)CoxAlyO 2 cathode for lithium-ion batteries during accelerated calendar and cycle life test. I. Comparison analysis between LiNi(1-x-y)Co xAlyO2 and LiCoO2 cathodes in cylindrical lithium-ion cells during long term storage test, J. Power Sources. 247 (2014) 412–422. https://doi.org/10.1016/j.jpowsour.2013.08.079.

[51] **C. Chu, L. Chang, D. Yin, D. Zhang, Y. Cheng, L. Wang,** Large-Sized Nickel-Cobalt-Manganese Composite Oxide Agglomerate Anode Material for Long-Life-Span Lithium-Ion Batteries, ACS Appl. Energy Mater. 4 (2021) 13811–13818. https://doi.org/10.1021/acsaem.1c02565.

[52] **W.S. Chen, H.J. Ho,** Recovery of valuable metals from lithium-ion batteries NMC cathode waste materials by hydrometallurgical methods, Metals (Basel). 8 (2018). https://doi.org/10.3390/met8050321.

[53] **M.T. Islam, U. Iyer-Raniga,** Lithium-Ion Battery Recycling in the Circular Economy: A Review, Recycling. 7 (2022). https://doi.org/10.3390/recycling7030033.

[54] **Z. Yu, H. Han, P. Feng, S. Zhao, T. Zhou, A. Kakade, S. Kulshrestha, S. Majeed, X. Li,** Recent advances in the recovery of metals from waste through biological processes, Bioresour. Technol. 297 (2020) 122416. https://doi.org/10.1016/j.biortech.2019.122416.

[55] **J. Alper,** The battery: Not yet a terminal case, Science (80-.). 296 (2002) 1224–1226. https://doi.org/10.1126/science.296.5571.1224.

[56] **G. Harper, R. Sommerville, E. Kendrick, L. Driscoll, P. Slater, R. Stolkin, A. Walton, P. Christensen, O. Heidrich, S. Lambert, A. Abbott, K. Ryder, L. Gaines, P. Anderson,** Recycling lithium-ion batteries from electric vehicles, Nature. 575 (2019) 75–86. https://doi.org/10.1038/s41586-019-1682-5.

[57] **J. Shaw-Stewart, A. Alvarez-Reguera, A. Greszta, J. Marco, M. Masood, R. Sommerville, E. Kendrick,** Aqueous solution discharge of cylindrical lithium-ion cells, Sustain. Mater. Technol. 22 (2019) e00110. https://doi.org/10.1016/j.susmat.2019.e00110.

[58] **O. Velázquez-Martínez, J. Valio, A. Santasalo-Aarnio, M. Reuter, R. Serna-Guerrero,** A critical review of lithium-ion battery recycling processes from a circular economy perspective, Batteries. 5 (2019) 5–7. https://doi.org/10.3390/batteries5040068.

[59] **R. Guo, L. Lu, M. Ouyang, X. Feng,** Mechanism of the entire overdischarge process and overdischarge-induced internal short circuit in lithium-ion batteries, Sci. Rep. 6 (2016) 1–9. https://doi.org/10.1038/srep30248.

[60] **S.E. Sloop, M. Allen,** Recycling and reconditioning of battery electrode materials. US 9484606 B1, J. Power Sources. 14 (2016) 145–149.

[61] **Y. Liu, D. Mu, R. Zheng, C. Dai,** Supercritical CO_2 extraction of organic carbonate-based electrolytes of lithium-ion batteries, RSC Adv. 4 (2014) 54525–54531. https://doi.org/10.1039/c4ra10530c.

[62] **S. Jin, D. Mu, Z. Lu, R. Li, Z. Liu, Y. Wang, S. Tian, C. Dai,** A comprehensive review on the recycling of spent lithium-ion batteries: Urgent status and technology advances, J. Clean. Prod. 340 (2022) 130535. https://doi.org/10.1016/j.jclepro.2022.130535.

[63] **B. Makuza, Q. Tian, X. Guo, K. Chattopadhyay, D. Yu,** Pyrometallurgical options for recycling spent lithium-ion batteries: A comprehensive review, J. Power Sources. 491 (2021) 229622. https://doi.org/10.1016/j.jpowsour.2021.229622.

[64] **L. Schwich, M. Küpers, M. Finsterbusch, A. Schreiber, D. Fattakhova-Rohlfing, O. Guillon, B. Friedrich,** Recycling strategies for ceramic all-solid-state batteries—part i: Study on possible treatments in contrast to li-ion battery recycling, Metals (Basel). 10 (2020) 1–19. https://doi.org/10.3390/met10111523.

[65] **P. Gautam, C.K. Behera, I. Sinha, G. Gicheva, K.K. Singh,** High added-value materials recovery using electronic scrap-transforming waste to valuable products, J. Clean. Prod. 330 (2022) 129836. https://doi.org/10.1016/j.jclepro.2021.129836.

[66] **G. Zhang, X. Yuan, Y. He, H. Wang, W. Xie, T. Zhang,** Organics removal combined with in situ thermal-reduction for enhancing the liberation and metallurgy efficiency of LiCoO2 derived from spent lithium-ion batteries, Waste Manag. 115 (2020) 113–120. https://doi.org/10.1016/j.wasman.2020.05.030.

[67] **Y. Tang, H. Xie, B. Zhang, X. Chen, Z. Zhao, J. Qu, P. Xing, H. Yin,** Recovery and regeneration of LiCoO2-based spent lithium-ion batteries by a carbothermic reduction vacuum pyrolysis approach: Controlling the recovery of CoO or Co, Waste Manag. 97 (2019) 140–148. https://doi.org/10.1016/j.wasman.2019.08.004.

[68] **J. Xiao, R. Gao, L. Zhan, Z. Xu,** Unveiling the Control Mechanism of the Carbothermal Reduction Reaction for Waste Li-Ion Battery Recovery: Providing Instructions for Its Practical Applications, ACS Sustain. Chem. Eng. 9 (2021) 9418–9425. https://doi.org/10.1021/acssuschemeng.1c02628.

[69] **G. Lombardo, B. Ebin, M.R.J. St Foreman, B.M. Steenari, M. Petranikova,** Chemical Transformations in Li-Ion Battery Electrode Materials by Carbothermic Reduction, ACS Sustain. Chem. Eng. 7 (2019) 13668–13679. https://doi.org/10.1021/acssuschemeng.8b06540.

[70] **J. Li, G. Wang, Z. Xu,** Environmentally-friendly oxygen-free roasting/wet magnetic separation technology for in situ recycling cobalt, lithium carbonate and graphite from spent LiCoO2/graphite lithium batteries, J. Hazard. Mater. 302 (2016) 97–104. https://doi.org/10.1016/j.jhazmat.2015.09.050.

[71] **R. Jha, M.D. Rao, A. Meshram, H.R. Verma, K.K. Singh,** Potential of polymer inclusion membrane process for selective recovery of metal values from waste printed circuit boards: A review, J. Clean. Prod. 265 (2020) 121621. https://doi.org/10.1016/j.jclepro.2020.121621.

[72] **M.D. Rao, K.K. Singh, C.A. Morrison, J.B. Love,** Challenges and opportunities in the recovery of gold from electronic waste, RSC Adv. 10 (2020) 4300–4309. https://doi.org/10.1039/c9ra07607g.

[73] **R.C. Wang, Y.C. Lin, S.H. Wu,** A novel recovery process of metal values from the cathode active materials of the lithium-ion secondary batteries, Hydrometallurgy. 99 (2009) 194–201. https://doi.org/10.1016/j.hydromet.2009.08.005.

[74] **J. Nan, D. Han, X. Zuo,** Recovery of metal values from spent lithium-ion batteries with chemical deposition and solvent extraction, J. Power Sources. 152 (2005) 278–284. https://doi.org/10.1016/j.jpowsour.2005.03.134.

[75] **B. Swain, J. Jeong, J. chun Lee, G.H. Lee, J.S. Sohn,** Hydrometallurgical process for recovery of cobalt from waste cathodic active material generated during manufacturing of lithium ion batteries, J. Power Sources. 167 (2007) 536–544. https://doi.org/10.1016/j.jpowsour.2007.02.046.

[76] **L. Sun, K. Qiu,** Vacuum pyrolysis and hydrometallurgical process for the recovery of valuable metals from spent lithium-ion batteries, J. Hazard. Mater. 194 (2011) 378–384. https://doi.org/10.1016/j.jhazmat.2011.07.114.

[77] **D.A. Ferreira, L.M.Z. Prados, D. Majuste, M.B.** Mansur, Hydrometallurgical separation of aluminium, cobalt, copper and lithium from spent Li-ion batteries, J. Power Sources. 187 (2009) 238–246. https://doi.org/10.1016/j.jpowsour.2008.10.077.

[78] **J. Wang, M. Chen, H. Chen, T. Luo, Z. Xu,** Leaching Study of Spent Li-ion Batteries, Procedia Environ. Sci. 16 (2012) 443–450. https://doi.org/10.1016/j.proenv.2012.10.061.

[79] **Z. Takacova, T. Havlik, F. Kukurugya, D. Orac,** Cobalt and lithium recovery from active mass of spent Li-ion batteries: Theoretical and experimental approach, Hydrometallurgy. 163 (2016) 9–17. https://doi.org/10.1016/j.hydromet.2016.03.007.

[80] **S. Castillo, F. Ansart, C. Laberty-Robert, J. Portal,** Advances in the recovering of spent lithium battery compounds, J. Power Sources. 112 (2002) 247–254. https://doi.org/10.1016/S0378-7753(02)00361-0.

[81] **E. Gerold, C. Schinnerl, H. Antrekowitsch,** Critical Evaluation of the Potential of Organic Acids for the Environmentally Friendly Recycling of Spent Lithium-Ion Batteries, Recycling. 7 (2022). https://doi.org/10.3390/recycling7010004.

[82] **L. Li, J. Lu, Y. Ren, X.X. Zhang, R.J. Chen, F. Wu, K. Amine,** Ascorbic-acid-assisted recovery of cobalt and lithium from spent Li-ion batteries, J. Power Sources. 218 (2012) 21–27. https://doi.org/10.1016/j.jpowsour.2012.06.068.

[83] **J. Kondás, J. Jandová, M. Nemeckova,** Processing of spent Li/MnO2 batteries to obtain Li_2CO_3, Hydrometallurgy. 84 (2006) 247–249. https://doi.org/10.1016/j.hydromet.2006.05.009.

[84] **S. Zhou, Y. Zhang, Q. Meng, P. Dong, Z. Fei, Q. Li,** Recycling of $LiCoO_2$ cathode material from spent lithium ion batteries by ultrasonic enhanced leaching and one-step regeneration, J. Environ. Manage. 277 (2021) 111426. https://doi.org/10.1016/j.jenvman.2020.111426.

[85] **L. Sun, K. Qiu,** Organic oxalate as leachant and precipitant for the recovery of valuable metals from spent lithium-ion batteries, Waste Manag. 32 (2012) 1575–1582. https://doi.org/10.1016/j.wasman.2012.03.027.

[86] **Z. Niu, Y. Zou, B. Xin, S. Chen, C. Liu, Y. Li,** Process controls for improving bioleaching performance of both Li and Co from spent lithium ion batteries at high pulp density and its thermodynamics and kinetics exploration, Chemosphere. 109 (2014) 92–98. https://doi.org/10.1016/j.chemosphere.2014.02.059.

[87] **Y. Qi, F. Meng, X. Yi, J. Shu, M. Chen, Z. Sun, S. Sun, F.R. Xiu,** A novel and efficient ammonia leaching method for recycling waste lithium ion batteries, J. Clean. Prod. 251 (2020) 119665. https://doi.org/10.1016/j.jclepro.2019.119665.

[88] **W. Wang, X. Zhang, C. Xin, Z. Rao,** An experimental study on thermal management of lithium ion battery packs using an improved passive method, Appl. Therm. Eng. 134 (2018) 163–170. https://doi.org/10.1016/j.applthermaleng.2018.02.011.

[89] **H. Ye, G. Zheng, X. Yang, D. Zhang, Y. Zhang, S. Yan, L. You, S. Hou, Z.L. Huang,** Application of different carbon-based transition metal oxide composite materials in lithium-ion batteries, J. Electroanal. Chem. 898 (2021) 115652. https://doi.org/10.1016/j.jelechem.2021.115652.

[90] **X. Zhu, J. Xiao, Q. Mao, Z. Zhang, Z. You, L. Tang, Q. Zhong,** A promising regeneration of waste carbon residue from spent Lithium-ion batteries via low-temperature fluorination roasting and water leaching, Chem. Eng. J. 430 (2022) 132703. https://doi.org/10.1016/j.cej.2021.132703.

[91] **Y. Yang, S. Lei, S. Song, W. Sun, L. Wang,** Stepwise recycling of valuable metals from Ni-rich cathode material of spent lithium-ion batteries, Waste Manag. 102 (2020) 131–138. https://doi.org/10.1016/j.wasman.2019.09.044.

[92] **L. Shuya, C. Yang, C. Xuefeng, S. Wei, W. Yaqing, Y. Yue,** Separation of lithium and transition metals from leachate of spent lithium-ion batteries by solvent extraction method with Versatic 10, Sep. Purif. Technol. 250 (2020) 117258. https://doi.org/10.1016/j.seppur.2020.117258.

[93] **M. Al-Gabalawy, N.S. Hosny, S.A. Hussien,** Lithium-ion battery modeling including degradation based on single-particle approximations, Batteries. 6 (2020) 1–26. https://doi.org/10.3390/batteries6030037.

CURRICULUM VITAE

Name Surname : Sepehr ABTAHI

EDUCATION:

- **B.Sc.** : 2011, Electronics engineering (honors), Multimedia university, Cyberjaya, Malaysia

PUBLICATIONS, PRESENTATIONS AND PATENTS ON THE THESIS:

- **Abtahi S.,** Benzeşik K., Turan A., Yücel O. "Recovery of Valuable Metals from Waste Lithium-ion Batteries by Metallurgical Routes", IMMC'2021 International Metallurgy & Materials Congress, in Digital Platform, 10-12 June 2021